PB93206225

NISTIR 5147

STRENGTH OF PARTIALLY-GROUTED MASONRY SHEAR WALLS UNDER LATERAL LOADS

S. G. Fattal

June, 1993

U. S. DEPARTMENT OF COMMERCE
Technology Administration
National Institute of Standards and Technology
Gaithersburg, MD 20899

Reproduced by:
National Technical Information Service
U.S. Department of Commerce
Springfield, VA 22161

NISTIR 5147

Strength of Partially-Grouted Masonry Shear Walls Under Lateral Loads

S. G. Fattal

U.S. DEPARTMENT OF COMMERCE
Technology Administration
National Institute of Standards
and Technology
Gaithersburg, MD 20899

NIST

NISTIR 5147

Strength of Partially-Grouted Masonry Shear Walls Under Lateral Loads

S. G. Fattal

U.S. DEPARTMENT OF COMMERCE
Technology Administration
National Institute of Standards
and Technology
Gaithersburg, MD 20899

June 1993

U.S. DEPARTMENT OF COMMERCE
Ronald H. Brown, Secretary

NATIONAL INSTITUTE OF STANDARDS AND TECHNOLOGY
Arati Prabhakar, Director

ACKNOWLEDGEMENT

The author acknowledges the contribution of Gregg Borchelt, Brick Institute of America, who critically reviewed the manuscript as Washington Editorial Review Board reader.

ABSTRACT

A proposed equation for estimating the strength of partially-grouted masonry shear walls failing in the shear mode is used to compare predicted strengths with the test results of 72 specimens from three experimental programs. The comparison shows that the predictions become less consistent with decreasing specimen strength and amount of reinforcement. Overall, predictions were within 20% of the test results for 50% of the specimens. For unreinforced walls and walls which had no vertical reinforcement, the predicted strength was less than half the test strength. It is shown that by altering the parametric functions in the predictive equation to represent more closely post-cracking resistance mechanisms in shear walls, the correlation of prediction with measured strength can be improved significantly.

Key Words: Building technology; masonry walls; predicted Strength; reinforced walls; shear strength; shear walls; measured strength.

UNITS

SI units are used in this report. U.S. Customary Units are also included as a supplement to recognize the state of current masonry practices in the U.S. Masonry codes and standards, construction specifications and tolerances, and nominal and actual sizes of standard masonry units manufactured in the United States are all specified in U.S. Customary Units.

CONTENTS

NOTATION

A = $(L)(t)$ = gross horizontal area of wall (mm^2)

A_n = net horizontal area of wall (mm^2)

A_h = area of uniformly distributed horizontal reinforcement in one course (mm^2)

A_{ve} = area of vertical reinforcement in one end cell (mm^2)

A_{vi} = area of vertical reinforcement in one interior cell (mm^2)

d = $L-d'$ = distance of centroid of vertical reinforcement in an end cell to the opposite face of wall (mm)

d' = distance from the centroid of vertical reinforcement in an end cell to the closer end face of wall (mm)

f_m = compressive strength of masonry from prism tests (MPa)

f_{yh} = yield strength of horizontal reinforcement (MPa)

f_{yv} = average yield strength of vertical reinforcement (MPa)

f_{yve} = yield strength of vertical reinforcement in exterior cells (MPa)

f_{yvi} = yield strength of vertical reinforcement in interior cells (MPa)

h = height of wall (mm)

L = length of wall (mm)

M = maximum bending moment that occurs simultaneously with shear force V (kN-mm)

Q = axial load on masonry wall (kN)

q = Q/A = nominal axial stress on wall (MPa)

r = h/L = aspect ratio of wall based on length L

r_d = $h/d = rL/d$ = aspect ratio based on effective depth d

s = deviation, as defined by Equation (2) (MPa)

s_h = spacing between layers of uniformly distributed horizontal reinforcement (mm)

s_{vi} = spacing of vertical reinforcement in the interior cells (mm)

t = thickness of wall (mm)

V = shear force on horizontal section of wall (kN)

V_u = ultimate shear force on horizontal section of wall determined by tests (kN)

v_a = variation, as defined by Equation (4)

v_m = contribution of ρ_v or ρ_{ve} and other parameters to predicted ultimate shear strength as defined by Equation (1) or (6) (MPa)

v_p = $v_m + v_s + v_q$ = predicted ultimate shear strength calculated by Equation (1) or (6) (MPa)

v_q = contribution of q to predicted ultimate shear strength as defined by Equation (1), or contribution of q and f_m to predicted ultimate shear strength as defined by Equation (6) (MPa)

v_s = contribution of ρ_h and other parameters to predicted ultimate shear strength as defined by Equation (1) or (6) (MPa)

v_t = V_u/tL = nominal ultimate shear strength based on test results (MPa)

X_m = sample mean as defined by Equation (3) (MPa)

α = $M/VLr = M/V_d r_d$ = a numerical coefficient dependent on, and satisfying equilibrium and boundary conditions

δ = numerical coefficient to account for the effect of boundary conditions in prediction of shear strength

γ = numerical coefficient as defined in Equation (1) and assigned values according to type of masonry, amount of grout, and type of test setup.

ρ_h = $A_h/(s_h)(t)$ = horizontal reinforcement ratio

ρ_v = $[(2A_{ve} + \Sigma(A_{vi})]/tL$ = total vertical reinforcement ratio

ρ_{ve} = A_{ve}/tL = ratio of vertical reinforcement in one end cell

ρ_{vi} = $A_{vi}/(s_{vi})(t)$ = ratio of uniformly distributed vertical reinforcement in the interior cells

Note: Because of limited font options in the software used, the notation in certain figures and tables are different from those above as follows:

fyh	=	f_{yh}	ph	=	ρ_h
fyv	=	f_{yv}	pv	=	ρ_v
fyve	=	f_{yve}	pve	=	ρ_{ve}
fyvi	=	f_{yvi}	pvi	=	ρ_{vi}
sh	=	s_h	rd	=	r_d
vm	=	v_m	vs	=	v_s
vt	=	v_t	vp	=	v_p
vu	=	v_u	vq	=	v_q

EXECUTIVE SUMMARY

This study examines the effectiveness of an equation proposed by Akira Matsumura (Equation 1, Section 3.2), and a modified version of that equation (Equation 6, Section 6), to determine the strength of masonry shear walls failing in the shear mode.

The basis of comparison are 72 tests of partially-grouted masonry shear walls from three experimental programs: 51 tests conducted by Matsumura at Kanagawa University in Japan; 11 by Chen et al. at the University of California, Berkeley; and 10 by Yancey et al. at the National Institute of Standards and Technology (NIST).

Equation (1) expresses the shear strength as the sum of three terms, designated herein by the symbols v_m, v_s, and v_q, which define the functional forms of the effects of specific parameters on strength. An earlier study examined the correlation of Equation (1) with the strength of 62 fully-grouted specimens from four experimental programs [2].

Equation (6) modifies the functional forms of the parameters in Equation (1) to obtain a closer correlation with the test results of the partially-grouted as well as the fully-grouted specimens. The functional forms of v_m and v_s are altered to simulate more closely observed mechanisms of shear wall behavior, and v_q is altered by the addition of a function to account for the effect of the compressive strength of masonry independent of the other parameters.

Section 1 gives a brief chronology of recent masonry research activities at NIST. Section 2 states the objective of this study to explore and improve the capability to predict the measured shear strength of masonry walls under reverse cyclic lateral loads. Section 3 introduces Equation (1) and describes the experiments, including the test setups, and tabulation of physical and material properties of the specimens.

Section 4 describes the development and reduction of the data into interpretable form. It includes tables and graphical presentations of predicted vs measured strengths, strength ratios vs test variables for specimens in which only one parameter varied, and statistical data for evaluating the correlations.

Section 5 interprets the data and draws conclusions on the adequacy of Equation (1) to predict shear strength.

Section 6 introduces Equation (6) and explains the rationale behind the modifications of the functional forms of certain parameters in Equation (1) to achieve closer correlation with the test results. The ratios of predicted-to-measured strengths, v_p/v_t, plotted in Figures 14-17, highlight the differences between the two equations.

For the 72 partially-grouted walls, strength predicted by Equation (1) varies from 23% to 180% of measured strength, with 46% falling within ±20% range. Predictions by Equation (6) vary from 41% to 146% of measured strength, with 68% falling within ±20% range.

For the 62 fully-grouted walls, strength predicted by Equation (1) varies from 53% to 135% of measured strength, with 74% falling within ±20% range. Predictions by Equation (6) vary from 47% to 128% of measured strength, with 82% falling within ±20% range.

The following conclusions are drawn from this study:

Equation (1) cannot predict the strength of unreinforced walls because it makes no provision for the effect of the compressive strength of masonry on shear capacity in the absence of reinforcement.

Equation (1) yields unreasonably low estimates of strength for walls in which only horizontal reinforcement is used.

The correlation of predicted strength with measured strength improves when the functional forms of certain parameters in Equation (1) are altered to simulate closely mechanisms of shear wall response.

Equation (6) is viewed as a first step. Additional measurements and observations of shear resistance mechanisms are needed to verify and improve further the modelling of the effects of the various parameters on strength.

1. INTRODUCTION

The National Earthquake Hazards Reduction Act (NEHRP) enacted by the U.S. Congress in 1977, and reauthorized in 1990 (P.L. 101-614), assigned the National Institute of Standards and Technology (NIST) the mission to carry out research and development to improve building codes and standards and practices for structures subjected to earthquakes. The NIST masonry research program is part of that mission. It calls for experimental and analytical studies of the response of masonry shear walls under simulated earthquake loads, in collaboration with studies carried out by the Technical Coordinating Committee for Masonry Research (TCCMAR), and its Joint U.S.-Japan component (JTCCMAR).

A recent NIST report titled "Review of Research Literature on Masonry Shear Walls" [1], examined the existing documentation on experimental research of masonry shear walls conducted during the past 15 years. A recommendation of that report is to evaluate the accuracy and reliability of formulations for predicting masonry shear wall strength under lateral and gravity loads. This recommendation was implemented in part by a study [2] which compared measured shear strengths of fully-grouted masonry walls with those calculated by four predictive equations.

The present study examines the correlation of predicted shear strengths of partially-grouted masonry shear walls by a proposed equation with the measured strengths of 72 specimens obtained from three test programs. Section 3 presents the proposed predictive equation and the data sets examined in this study. Section 4 describes the reduction of data into interpretable form. Section 5 presents the analysis of the results of the comparative study for partially-grouted walls. Section 6 presents the methodology used in the derivation of an improved predictive equation, and its correlation with test results of both fully-grouted and partially-grouted walls. Conclusions drawn from this study are summarized in Section 7.

2. OBJECTIVE

The objective of this study is to evaluate, and, if necessary, to improve, the analytical capability to predict measured shear strength of masonry walls subjected to reverse cyclic lateral loads.

3. SCOPE

The study reported in Reference 2 examined the correlation of predicted strength with the test results of 62 fully-grouted reinforced specimens. This study focuses on the correlation of strength predictions with available test results of 72 partially-grouted and unreinforced specimens. First, a proposed equation is used to develop data for comparison with the test results. Next, the functional forms of the parameters in the proposed equation are modified according to known mechanisms of shear wall response, to obtain a closer correlation with the measurements of partially-grouted, ungrouted, and fully-grouted specimens.

The experimental data were selected from about 700 independent tests of masonry shear walls identified and documented in a separate report [1]. The selection was based on common aspects and features of the experimental programs, i.e., boundary conditions, test setup, load cycling procedure, physical similarities, choice of parameters, etc. The test results of 62 fully-grouted specimens described in an earlier study [2], and 72 partially-grouted specimens described in this study, are used as basis of the comparisons presented in this study.

3.1 Experimental Data Sets

All the partially-grouted masonry specimens selected for this study were tested with the two opposite surfaces (parallel to the bed joints) kept rotationally fixed or parallel. They were subjected to increasing reverse cyclic lateral displacements until failure in the shear mode was reached. Both concrete block and clay masonry specimens are included. The three sets of data are identified by the letters M, B, and N, respectively, in this report.

SET M:

Fifty one specimens were selected from tests conducted by Matsumura at Kanagawa University in Japan [3,4].

SET B:

Eleven specimens were selected from test program at University of California, Berkeley, California, conducted by Chen et al. [5] and Hidalgo et al. [6].

SET N:

Ten specimens tested at the National Institute of Standards and Technology (NIST) by Yancey and Scribner [7].

In all the tests, displacement-controlled multiple cycles of reversed loadings were used according to predefined load-displacement histories, characterized by increasing amplitudes to failure. Loading procedures and loading rates of the three sets of specimens were similar. The test data include two maximum shear stresses for each specimen, corresponding to the two opposite directions of cyclic loading. Ultimate shear strength is taken as the average of these two maximum stresses. Specimens which were reported to have failed in flexure are excluded. Detailed definitions of load-displacement histories can be found in the cited references.

The specimen properties are listed in Table 1. The notation is defined at the front of this report. Data set M consists of specimens built with concrete block and clay brick units. Two types of test setups were used in these experiments: the "wall type" and "beam type", as shown in Figure 1. In wall-type experiments, the walls were tested in the upright configuration (bed joint horizontal), with the top and bottom surfaces kept rotationally fixed during testing. In the beam-type specimens, the masonry walls were flanked at the top and bottom surfaces by integrally-built reinforced concrete walls of equal height. These "wall-beams" were placed horizontally on edge (bed joint vertical) between four points of contact, two at the ends and two at the concrete-masonry junctions. Lateral displacement was effected by equal vertical movement of the second and fourth contact points in unison, the first and third contact points acting as reaction supports.

Beam-type tests produce a radially symmetric displacement field with respect to the geometric center of the masonry wall where the top and bottom surfaces remain parallel and rotate equally, i.e., they are elastically constrained against rotation. Therefore, lateral displacement under a given load will be greater than that for a wall having rotationally fixed boundaries, i.e., a beam-type wall is more flexible.

In Table 1 the concrete block specimens of data set M are identified by CW (wall type; tests 1-29) or CN (beam type; tests 30-39) in their designation. For brick walls WS4-M and WS4-B-M (tests 40 and 41), wall-type tests were used. Beam-type tests were used for the rest of the brick specimens (tests 42-51), including the small size specimens which are designated by the NS prefix.

All the tests of data set B (tests 52-62) were performed using wall-type procedure. Concrete block and brick specimens are identified by prefixes BL and BR, respectively. Specimens BL2P-B and BR2P-B were unreinforced.

The N series tests (nos. 63-72) were performed using concrete block specimens and the wall-type procedure. One wall, R1-N (test 63), was unreinforced. The rest contained only horizontal reinforcement.

The subsequent columns of Table 1 specify respectively, wall dimensions (h, L, t, and d); spacing of horizontal reinforcement (s_h); yield strengths of horizontal and vertical reinforcement (f_{yh}, fy_{ve}, f_{yvi}, and f_{yv}); exterior, interior and total vertical reinforcement ratios (ρ_{ve}, ρ_{vi}, and ρ_v); horizontal reinforcement ratio (ρ_h); dual definitions of aspect ratio (r and r_d); axial stress (q); and compressive strength of masonry (f_m).

The compressive strength of the masonry was obtained by prism tests. The notation f_m is used to distinguish it from code-specified design strength f'_m which incorporates a correction factor dependent on the h/t ratio of the prism and on the type of masonry; concrete block or clay brick. Three-course prisms were used with test series M. Three-course and six-course prisms with h/t ratios of 2 and 4, respectively, were used with test series B. The listed strengths are the averages of the two. Three-course prisms were used with test series N.

3.2 Prediction of Shear Strength

The literature review [1] identified an equation, proposed by Matsumura [3,4], for estimating the ultimate in-plane shear strength of both fully-grouted (FG) and partially-grouted (PG) masonry walls in which shear is the dominant mode of failure. The equation is rearranged below to reflect the sum of three groupings of parameters as follows:

$$v_p = v_m + v_s + v_q$$

$$= \{[(0.76/(r_d + 0.7) + 0.012)(4.04)(\rho_{ve})^{0.3}(k_u)(f_m)^{0.5}]\}(d/L)$$

$$+ [0.157(\rho_h \cdot f_{yh})^{0.5}(\gamma)(\delta)(f_m)^{0.5}](d/L)$$

$$+ [0.175(q)](d/L) \qquad (1)$$

where, v_m, v_s, and v_q, defined in the Notation Section, represent the three additive terms in Equation (1), respectively; v_p is the shear strength; and,

k_u = 1.00 for FG concrete and brick masonry and PG beam-type brick masonry

k_u = 0.80 for PG wall-type brick masonry and PG beam-type concrete masonry

k_u = 0.64 for PG wall-type concrete masonry

γ = 1.00 for FG concrete and brick masonry and PG brick masonry
γ = 0.60 for PG concrete masonry

δ = 1.00 for wall with inflection point at mid-height
δ = 0.60 for wall under cantilever-type loading.

The other terms in equation (1) are defined in the Notation Section at the front of this report.

4. DATA REDUCTION

The shear strength of the 72 test specimens were evaluated using Equation (1) and the properties listed in Table 1. The predicted-vs-measured strength results for the three data sets, M, B, and N, are presented individually as well as collectively in Figures 2-5. Figures 2(a) and 2(b) are additional plots for the concrete block and brick specimens of data set M, respectively.

The broken and solid lines shown in each plot represent, respectively, the perfect correlation line and the regression line $y = cx$, where c is a numerical constant. The spread of points above and below the broken line indicates high and low estimates of test strength, respectively, as well as inherent scatter of test results.

For each plot, deviation s, sample mean x_m, and variation v_a were calculated using the equations

$$s = [\ \Sigma\ (x_i - y_i)^2 / (n-1)\ ]^{0.5} \quad (i + 1...n) \quad \ldots\ldots\ldots \quad (2)$$

$$x_m = \Sigma\ x_i / n \quad \ldots\ldots\ldots\ldots\ldots\ldots\ldots \quad (3)$$

$$v_a = s / x_m \quad \ldots\ldots\ldots\ldots\ldots\ldots\ldots \quad (4)$$

where x_i = i-th test value, y_i = i-th predicted value, and n = sample size.

Equation (2) is similar to the expression for standard deviation but the numerical value of the deviation cannot be used in statistical analysis because data points being evaluated do not represent repetitive tests and the scatter is due to multiple causes. Likewise, variation, Eq. (4), is defined the same way as coefficient of variation in statistics (standard deviation divided by the sample mean), but for the same reasons, does not have the

same meaning. However, as defined and calculated here, these indicators are useful in making comparisons of the relative accuracy of predictions for the individual data sets, assuming variability in test results can be estimated.

Information on replicate shear wall tests is scarce. A study by Blume and Proulx [8] gives an indication of the magnitude of inherent variation that can be expected in tests of masonry shear walls of comparable size (1.22 X 1.22-m or 4 X 4-ft two-wythe grouted brick specimens). Test results from 84 diagonally-loaded specimens in replicate groups of four and five, gave a range of 3-18% on the coefficient of variation. The large spread in the coefficient of variation is attributed primarily to small sample sizes. The average coefficient of variation for all the replicate tests was 8%.

Table 2 lists statistical data for nine groups of duplicate tests belonging to data set M. The spread from duplicate averages was 0 to ±14%, with an average spread of ±2.7%.

Table 3 specifies the contribution of each of the three terms, v_m, v_s and v_q, to the predicted strength v_p calculated by Equation (1). The measured strengths are listed in the last column of the same table. For data set M, the ratios v_m/v_p, v_s/v_p, v_q/v_p, and v_p/v_t, where v_t is the measured strength, are plotted in Figure 6 against test numbers 1-51. Figures 7 and 8 show similar plots for data sets B (test nos. 52-62) and N (test nos. 63-72), respectively. These plots are used to identify conflicting trends in predicted strengths for groups of specimens sharing common physical properties.

Data set M contains groups of specimens that essentially differed in one parameter only. Section 5.1 includes tables which identify the specimens in each group and specify the corresponding fixed and variable parameters (q, r, f_m, and ρ_h). There were no groups in which only parameter ρ_{ve} varied. In Figures 9-12, the ratios of predicted-to-measured strengths are plotted against the variable parameters to examine the accuracy of their functional forms in Equation (1). Figure 13 has been prepared to assist the interpretation of data for the specimens belonging to each group. It contains the same information as in Figure 6 except the data points are rearranged according to the groups. Specimens which do not belong a group are excluded.

In Section 6, Equation (1) is modified based on mechanisms of shear wall behavior and insight gained from its comparative evaluation against test data. The modified equation is checked against the results of the same 72 tests of PG walls, as well as against the test results of 62 FG walls examined in another study [2]. Figures 14 and 15 display the data points of the v_p/v_t ratios for the PG

walls based on Equations (1) and (6), respectively. Figures 16 and 17 display the v_p/v_t ratios for the 62 FG walls based on Equations (1) and (6), respectively. The two sets of figures offer a quick visual assessment of the improvements.

5. ANALYSIS

5.1 M-M comparison

In this report, the format X-Y, where X is the equation identification, and Y is the data set, is used for the comparisons. For example, M-B refers to the comparison of the predictions by Matsumura's equation (1) with test results of data set B. In Figure 2, the predicted strengths according to Equation (1) are plotted against the results of 51 tests of set M. It shows predicted strength exceeds measured strength by about 9%. The deviation is 0.19 MPa (27.5 psi) which is 23% of the mean strength (v_a = 0.23, Table 4). Agreement between prediction and measurement appears to improve with increasing test strength. This trend becomes easier to detect when separate comparisons are made for the concrete block and clay brick specimens, as shown in Figures 2(a) and 2(b), respectively. The deviation for the brick specimens is 0.24 MPa (35 psi), which is 17% of the mean test strength. The comparative figures for the concrete block specimens are, 0.17 MPa (25 psi) and 28%, respectively. When a correction factor of 0.92, the reciprocal of the regression constant, is applied to equation (1) as a multiplier, the correlation improves accordingly, as indicated in Table 4. However, the accuracy of equation (1) so improved, will have to be examined for consistency against other test data.

The ability of an equation to predict strength depends on accurate representation of the effect of the parameters on response. Both the weights of the parameters and their interactions need to be examined in relation to test results to evaluate the accuracy of their functional forms. Equation (1) may be expressed in terms of six parametric functions as follows:

$$\begin{aligned} v_p &= v_m + v_s + v_q \\ &= f_1(r) \cdot f_2(\rho_{ve}) \cdot f_3(f_m) \\ &\quad + f_4(\rho_h) \cdot f_5(f_{yh}) \cdot f_3(f_m) \\ &\quad + f_6(q) \qquad \text{..... (5)} \end{aligned}$$

where,

$$f_1(r) = \{[0.76 / (r_d + 0.7)] + 0.012\}.(d/L)$$

$$f_2(\rho_{ve}) = 4.04(k_u)\ (\rho_{ve})^{0.3}$$

$$f_3(f_m) = (f_m)^{0.5}$$

$$f_4(\rho_h) = 0.157(\rho_h)^{0.5}(\gamma)(\delta)(d/L)$$

$$f_5(f_{yh}) = (f_{yh})^{0.5}$$

$$f_6(q) = 0.175(q)\ .\ (d/L)$$

In Figure 6, the non-dimensional terms v_m/v_p, v_s/v_p, v_q/v_p, and v_p/v_t are plotted against test numbers as specimen identifiers. The first three terms show the contributions of v_m, v_s and v_q, respectively, to predicted strength v_p (their sum is equal to one). The fourth term, v_p/v_t, where v_t represents the measured strength, indicates deviation of predicted strength from measured strength.

There are 33 specimens without axial load (Nos. 1-11 and 30-51, Fig. 6). For these specimens, $q = f_6(q) = v_q = 0$, and, therefore, $v_p = v_m + v_s$. Among them, nine specimens have no horizontal reinforcement (Nos. 7, 8, 30-33, 36, 37, 42), so that $\rho_h = f_4(\rho_h) = v_s = 0$, and $v_p = v_m = f_1(r).f_2(\rho_{ve}).f_3(f_m)$.

Now examine these specimens closer, using the groupings in Table 5. Equation (1) overestimated the strength of specimens 7 and 8 of group A by 80 and 45%, respectively. Their strengths, 0.30 and 0.37 MPa (43 and 53 psi, Table 3), respectively, are at the lower end of the strength range (0.30 to 0.96 MPa or 43 to 139 psi) of the 39 concrete block specimens (nos. 1-39). Predictions for brick specimens 30 and 31 of group B, at the higher end of the test range, 0.72 and 0.96 MPa, or 105 and 139 psi, respectively, were much closer to test strength (v_p/v_t = 1.2 and 0.9, respectively). All other values being essentially the same for the two groups (Table 5), the discrepancy indicates the inaccuracy of the function representing the effect of ρ_{ve} on strength of concrete block specimens in Equation (1);

$$f_2(\rho_{ve}) = 4.04(k_u)(\rho_{ve})^{0.3}$$

The function places excessive weight on the effect of ρ_{ve} for specimens in which relatively light vertical reinforcement is used.

Specimens in groups B and C differ essentially in r only, while those in groups A and C differ in both r and ρ_{ve}. The predictions for the specimens in group B and C are close to their respective strengths while the predictions for the specimens in group A are

well over their measured strengths. The specimens in groups A and C developed lower strengths than those in group B (the measured test strengths of group C were in the range of 0.37 to 0.49 MPa or 54 to 71 psi). These results imply an inherent inaccuracy in the function $f_1(r)$ as well, in modelling the effect of aspect ratio on strength, i.e., the error in f_1 compensated for the error in f_2 so that group C predictions were close to test results.

The above example illustrates the difficulty in completely isolating the effect of each parameter on strength. Alternatively, the response of groups of specimens having almost identical properties except in one parameter, was examined.

Figures 9-12 have been developed for this purpose, using the information contained in Tables 5-9. They exhibit the effect of variables q, r, ρ_v, and f_m, respectively. In each figure, the ratio of predicted-to-measured strengths, v_p/v_t, is plotted against the variable parameter. The legend identifies the different groups in each plot. For example, Figure 10 identifies six groups, each of which have common properties except in parameter r. Figure 13 duplicates the data in Figure 6, except the tests identified by their numbers along the x axis are rearranged in the sequence of the four variables addressed in Figures 9-12. Tests which do not belong to any group are not included in the plot.

In Figures 9-13, the specimen identifiers (test numbers) are not used. However, the data points in each group are plotted in the order of increasing value of the variable parameter as given in Tables 5-9.

(A). Effect of Axial Load, q

Figure 9 shows the results of four tests in which axial load was the only variable. The measured strength v_t, predicted strength v_p, and their ratio v_p/v_t are plotted against axial load q. Table 6 specifies the values of the fixed parameters and variable q for this group.

For a perfect correlation of an effect (axial stress q, in this case), the data points representing the strength ratio v_p/v_t should fall on a horizontal line having an ordinate of unity. The combined effect of the fixed parameters in a group is the "default" case of the variable parameter. The default case for parameters q, ρ_h, and ρ_v is zero. For example, the default case q = 0 indicates that the combined effect of the four other parameters, having the values specified in Table 5, is a predicted strength which exceeds measured strength by 42%. A meaningful indicator of the error in the formulation of a parametric effect is the slope m of the linear

regression curve $y = mx + b$ for the data points representing the strength ratios. The slope of the regression line for the strength ratios plotted in Figure 9 is 0.108 $[MPa]^{-1}$, indicating close agreement between predicted and measured strengths. This is further verified by comparing the slopes of the v_p curve and the regression line of the data points representing the measured strengths v_t (0.175 vs 0.191, respectively).

Although the axial load function $f_6(q)$ seems to correlate well with these tests, it needs to be verified against a larger sample, preferably against groups sharing sets of fixed parameters having different values from those of this group. The need for such additional data is indicated in the discussions which follow.

(B). Effect of Aspect Ratio, r

The effect of aspect ratio is shown in Figure 10. There are six groups of specimens in which only r varied. The fixed parameters in each group have different values from those in the other groups as specified in Table 7.

The predicted strength of specimens in group 1 (test nos. 2,4,6) is the sum of v_m and v_s in Equation 5 (v_q = 0, Figure 13). The strengths of these specimens are overestimated by substantial margins (about 30-60%). Since any one or a combination of the functions f_1-f_5 (of r, ρ_{ve}, f_m, ρ_h, f_{yh}) in v_m and v_s of Equation 5 may contribute to overprediction of test strength for this group, it is impossible to suspect a specific parametric function on the basis of the spread between the predicted and measured strengths.

The significant aspect of the results shown in Figure 10 is the change in the strength ratio v_p/v_t relative to the change in the variable parameter r. For group 1, the strength ratio decreases sharply with increasing r. As r increases from 1 to 2, v_p/v_t drops from 1.6 to 1.3. Obviously, function $f_1(r)$ is not a good model for the set of fixed parameters of group 1.

Groups 2 and 3 also show v_p/v_t decreases with increasing r, but at a slower rate, which implies that $f_1(r)$ is a better model for the fixed parameters in these groups. Groups 1 and 3 differ only in f_m and ρ_{ve}. If the compressive strength of group 3 were used, the calculated stresses of group 1 would be lower by about 22% but the characteristic shape of the v_p/v_t-vs-r curve will not change. This implies that f_1 does not adequately describe the effect of r when the vertical reinforcement ratio is low, as in group 1 specimens.

Group 4 exhibits mixed results while those of groups 5 and 6 exhibit a trend opposite to Groups 1 and 2. The average strengths of groups 1-4 are less than the average strength of the 51

specimens (Table 3), while those of groups 5 and 6 are well above the average strength; a possible reason for the conflicting effects noted above. Overall, the strength ratio decreases with increasing r as indicated by the regression line for all the data points shown in Figure 10.

The above results question the effectiveness of the functional form of parameter r in Equation (1). There is no obvious reason for $f_1(r)$ to be coupled only to the v_m term. Function f_1 increases at an increasing rate with decreasing r. This implies that the effect of r on predicted strength is too high for specimens of low aspect ratio, or too low for those having a high aspect ratio, or both.

(C). Effect of Horizontal Reinforcement, ρ_h

Figure 11 shows the effect of horizontal reinforcement ratio, ρ_h, on strength. There are six groups in this category, each having nearly identical parameters except ρ_h, as specified Table 8. All five specimens in group 1 have no axial load ($v_q = 0$). In addition, specimens 7 and 8 are duplicates and have no horizontal reinforcement ($v_s = 0$). The strengths of all five specimens in this group are well overpredicted by 40-80%. In particular, since $v_p = v_m$ for specimens 7 and 8, the high estimate is an indication of excessive weight placed on the contribution of v_m to predicted strength.

According to Table 3, the specimens of Group 1 developed considerably lower strength than the average strength of the 51 tests (0.82 MPa or 118 psi). As ρ_h increased from 0 to 0.0022, the measured strength for the group increased from 0.30 to 0.56 MPa (43 to 81 psi), while the strength ratio v_p/v_t decreased from 1.8 to 1.4. Groups 2, 4 and 5 exhibit a similar trend. These results imply that excessive weight is placed on the effect of horizontal reinforcement on the strength of lightly-reinforced walls, or insufficient weight is placed on its effect on more heavily reinforced walls, or both.

Specimens in groups 3 and 6 (except No. 22, $v_t = 0.85$ MPa or 123 psi, Table 3) developed higher than the average strength of the 39 concrete block specimens (0.63 MPa or 92 psi). The effect of horizontal reinforcement on predicted strength was reasonably consistent for these two groups, i.e., v_p/v_t is less sensitive to variation in ρ_h). The general trend for all the data points (Figure 11) indicates v_p/v_t decreases with increasing ρ_h, as confirmed by the regression line shown in Figure 11.

(D). Effect of Compressive Strength, f_m

There are two groups of two specimens each, in which f_m varied, as indicated in Table 9. Figure 12 shows the relationship of v_p/v_t and compressive strength, f_m, which appears in both v_m and v_s expressions of Equation 1. The figure exhibits a mixed trend and lacks significance because of the small sample size.

Figures 6 and 13 show the relative importance of the three terms, v_m, v_s, and v_q, in Equation (1). The maximum contribution comes from v_m, which accounts for 50-100% of predicted strength; followed by v_s (20-40%) and v_q (0-20%). The compressive strength function, f_3, is common to both v_m and v_s terms, and the yield strength function, f_5, is constant because the steel bars used in all the specimens have the same yield strength. Thus the contribution of v_m comes from the product $f_1.f_2$ of the two parametric functions in r and ρ_{ve}, respectively, while the contribution of v_s comes from function f_4 in parameter ρ_h. Changes in the forms of these three functions for the purpose of improving correlation with the test data are discussed in the next Section.

In summary, Equation (1) exhibits a general tendency to overestimate test results. The trend is more dominant for walls which developed shear strengths at the lower end of the measured strength range. This non-conservative aspect of Equation (1) casts doubt about its reliability to predict lower strengths; around 1.04 MPa (150 psi) or less (Figure 2).

There is no evidence that the effect of aspect ratio r on strength is properly modeled, and whether or not it should be associated only with the v_m component of predicted strength. There is partial evidence to indicate that the function defining the effect of r lacks the consistency to account for the effect of aspect ratio on strength in the range of the test strengths examined.

There is also some evidence to indicate that the effect of both vertical and horizontal reinforcement can be significantly overestimated in lightly-reinforced walls.

5.2 M-B Comparison

Experimental data on partially-grouted masonry shear walls built in accordance with U.S. masonry construction specifications are scarce. Data set B (the Berkeley tests) consists of eight PG specimens of r = 1.17, and three PG specimens of r = 1.90 (Nos 52-59 and 60-62, respectively, Table 1). Specimens 52 and 56 were unreinforced. Specimens 54, 58, and 60 contained vertical reinforcement only.

In Figure 3 the predicted strengths of these eleven walls are plotted against their test results. The correlation is weaker than that for the M series as evidenced by a deviation which is almost one-third of the mean test strength (0.26 MPa or 37 psi, Table 4). The scatter is caused mainly by the poor results in the predicted strengths of the two unreinforced specimens (nos. 52 and 56) and the three specimens of the higher r series (nos. 60-62).

Figure 7 shows the strength ratios v_m/v_p, v_s/v_p, v_q/v_p, and v_p/v_t, for each specimen in data set B. The specimens are identified by the test numbers shown along the horizontal axis. The strengths of specimens 60-62 are overpredicted by 34-44%. At the other extreme, the predicted strengths of specimens 52 and 56 were 25 and 43% of the respective measured strengths. As indicated in Table 4, the correlation improves by leaving out the two unreinforced walls, nos.52 and 56 (v_a reduces from 0.33 to 0.27).

The poor correlation for the two unreinforced walls highlights another deficiency of equation (1). As $v_m = v_s = 0$ for both walls, $v_p = v_q$. However, v_q depends only on parameter q, axial stress. This leads to the ambiguous conclusion that a unreinforced masonry shear wall without axial load has no shear resistance under lateral load.

The linear expression $v_p = a + bq$, where a and b are numerical constants, has been commonly used to estimate the strength of unreinforced masonry shear walls. The numerical constants have been evaluated by calibration against experimental data of walls having different aspect ratios and compressive strengths [9, 10]. Without an additional term in the v_q expression to account for the contribution of f_m and r on unreinforced wall strength, the error in estimated strength becomes excessive for unreinforced walls. For lightly-reinforced walls below some minimum values of ρ_{ve} and ρ_h, predictions of the test results of data set B improved after eliminating the two unreinforced walls (Nos. 52 and 56) and the three (Nos. 60-62) having the higher aspect ratio. These predictions come to within ±12% of measured strength (Figure 7 and Table 4). This is closer than the correlation with the results of the concrete block masonry tests of data set M, even though both data sets had similar ranges of measured shear strength.

5.3 M-N Comparison

Data set N, the NIST tests, consists of 10 partially-grouted concrete block specimens (Nos. 63-72) which contained only horizontal reinforcement. The test variables were the amount, type, and distribution of the horizontal reinforcement, which consisted of steel bars and/or joint reinforcement. The steel bars were hooked at the ends and were placed at mid-height or at third

points in grouted bond beams. Two sizes of joint reinforcement were used, placed in each course or in every other course. Specimen 63 was unreinforced. Specimens 64 and 65 contained only joint reinforcement. Specimens 66-68 and 72 contained only reinforcing bars. Specimens 69-71 contained both steel reinforcing bars and joint reinforcement. The dimension of the specimens, h, t, and L, were identical to the concrete block (CB) specimens 52-55 of data set B.

Table 10 lists selected data for the specimens of data sets B and N. A constant axial load, corresponding to an axial stress of 0.74 MPa (107 psi) on the gross area, was maintained on all the specimens of data set N during testing. This is within the range of axial stresses in CB specimens 52-55 of data set B (range = 0.57-0.79 MPa or 83-115 psi; ave. = 0.63 MPa or 91 psi). The average prism strength of set N was lower than set B, at 7.91 MPa or 1146 psi (range = 5.91-8.91 MPa or 856-1292 psi), compared to 12.03 MPa or 1743 psi (range = 9.17-13.14 MPa or 1330-1905 psi) of CB specimens 52-55 of set B. The horizontal steel ratio of set N was 0-0.0021 versus 0-0.0015 for specimens 52-55 of set B. The average test strength was 0.66 MPa or 95 psi (range = 0.48-0.83 MPa or 70-121 psi) versus 0.75 MPa or 108 psi (range = 0.48-0.92 MPa or 69-133 psi) for specimens 52-55 of data set B. Thus, except for lower f_m and no vertical reinforcement, the specimens and test results of data set N are comparable to specimens 52-55 and test results of data set B.

Figures 4 and 8 clearly show that Equation (1) cannot predict the results of any test of data set N. Consider, first, the case of the unreinforced wall (no. 63). The predicted strength of this wall was 23% of the measured strength (0.48 MPa or 70 psi, Figure 8). Similar results occurred in the unreinforced wall tests 52 and 56 of data set B, which lends further support to the argument stated earlier, that Equation (1) does not adequately describe the effect of axial load on the strength of unreinforced walls because it does not account for the contribution of f_m in the absence of reinforcement.

Consider next the remaining nine reinforced walls in data set N. According to the results shown in Table 10 and Figure 8, the relative contributions of horizontal and vertical reinforcement are not modelled well in Equation (1). Although the test results of the specimens in data sets B and N are comparable, predictions for specimens in data set N are well below those of data set B. Predictions for the six specimens, 53-55 and 57-59, of data set B (the two unreinforced walls are excluded), closely match their test results. For example, compare no. 53 of set B with nos. 68 and 72 of set N. ρ_h and v_q are about the same. The values of v_s are different due to the differences in f_m. However, using the higher f_m (12.65 MPa or 1833 psi) will increase v_s of nos. 68 and 72 by only 0.03 MPa (5 psi).

Since in no. 53 the major contribution to predicted strength comes from v_m (0.46 MPa or 67 psi), and noting that $v_m = 0$ for nos. 68 and 72, it is concluded that the weight given to v_s relative to v_m in equation (1) is not adequate in modelling the effect of horizontal reinforcement, particularly when no vertical reinforcement is used. If more weight is given to v_s, the weight to v_m will have to be reduced accordingly. The results of tests 55, 59 and 60 of data set B (Table 10) show evidence that Equation (1) may be overestimating the effect of v_m.

5.4 Summary

Comparison with the test results of 51 specimens of data set M shows reasonably close correlation between predicted and measured strength for specimens which developed high strengths. As test strength decreased, both scatter and a tendency to overestimate strength increased (Figures 2, 2a, 2b).

Equation (1) cannot provide reasonable estimates of strength for walls without vertical reinforcement (tests 64-71 of data set N, Figure 8 and Table 10). Experimental evidence indicates that this may be attributed to the relative weights given to the v_m and v_s terms in the equation (typically, v_m/v_s is in the 2 to 4 range for both partially and fully grouted walls [2]).

Equation (1) cannot predict the shear strength of unreinforced walls (specimens 52, 56, 63). Since both v_m and v_s are zero for unreinforced walls, the predicted strength becomes a function of axial load only. This means, according to Equation (1), unreinforced walls without axial load will have no shear resistance. Thus, an additional function is needed, possibly coupled with the axial stress function, to account for the contribution of the non-zero parameters f_m and r on the shear strength of unreinforced walls.

Using groups of specimens in which only one parameter varied, deficiencies in the functional models of the effects of parameters of r, ρ_v, and ρ_h in Equation (1) were highlighted.

6. IMPROVEMENTS

In Section 5, the accuracy of an empirical equation to predict the strength of partially-grouted masonry shear walls was examined relative to the results of 72 independent tests. The comparison highlighted poor correlation with some of the test results. This was mainly attributed to inconsistencies of the functions

describing the effect of such parameters as axial load, aspect ratio, and the amounts of horizontal and vertical reinforcement on strength, over the range of values of these parameters that were used as test variables.

This Section discusses the effect of altering the functional forms of certain parameters for the purpose of improving the correlation of strength predictions with measured strength. The methodology involves the representation of parametric effects based on post-cracking mechanisms of shear wall response and the use of calibration against specific test results. The following equation is derived by substitution of new parametric functions in sequence and calibration of numerical constants against specific test results in each step.

$$
\begin{aligned}
v_p &= v_m + v_s + v_q \\
&= k_o.k_u.[(0.5/(r+0.8))+0.18].(f_m)^{0.5}(f_{yv})^{0.5}.(\rho_v)^{0.7} \\
&\quad + k_o.(0.011).(\gamma).(\delta).f_{yh}.(\rho_h)^{0.31} \\
&\quad + k_o.(0.012).(f_m)+(0.20).(q) \qquad \ldots\ldots\ldots\ldots\ldots\ldots\ldots\ldots (6)
\end{aligned}
$$

where k_0 = 0.8 for PG walls, 1.0 for FG walls.

The steps in the derivation of equation (6) will be described and the rationale behind each change will be explained. But the interim results will not be shown.

6.1 Modification of v_m

The first step involved the substitution of a new expression for the effect of vertical reinforcement on strength. It has been reported that vertical bars provide post-cracking resistance mainly through dowel action [11,12]. Priestley [12] has derived an equation for dowel action that has the functional form

$$v_d = k.\rho_v.(f'_b.f_{yv})^{0.5}$$

where v_d is the resistance of vertical reinforcement through dowel action, f'_b is the bearing strength of the grout, and coefficient k is a numerical constant. Note that this equation assumes that all vertical bars contribute to resistance through dowel action and not just the exterior bars as assumed in the derivation of equation (1).

At this step three assumptions are introduced as follows.

(a) A linear relation can be established between the bearing strength of grout and compressive strength f_m of masonry.

(b) The effectiveness of vertical reinforcement increases at a decreasing rate with increasing reinforcement.

(c) The effectiveness of vertical reinforcement decreases with increasing aspect ratio.

The validity of the first assumption may be examined by conducting appropriate bearing tests and companion compression tests of grouted prisms. The second assumption allows the use of an exponent less than one ($k_v < 1$) for ρ_v. A plausible explanation for the third assumption is that as diagonal cracks become steeper with increasing aspect ratio, the bearing block (viz. a wedge of grout) between the crack opening and the vertical bar across that opening becomes narrower, causing a decrease in bearing capacity.

The new expression for v_m in Equation (6) reflects these assumptions. The function $f_1(r)$ is retained but the three constants in that function as well as the exponent $k_v = 0.7$ of ρ_v have been evaluated through calibrations against the test results of specimens for which the v_p/v_t ratio is one or close to one, and none of the v_m, v_s, and v_q terms is zero. In effect, the selected tests are used as pivot before the next change is introduced. Constant k_o, common to all three terms of Equation (6), is a reduction factor for partially-grouted masonry to account for the effect of ungrouted cells. Its value is determined in the final step of the derivation by calibration against all the test results to minimize deviation s. It would have been preferable to determine k_o independently (e.g., $k_o = V_n/V_g$, where V_n and V_g are the volumes of partially and fully grouted wall, respectively), and check its validity against all the test results. However, available information was not sufficient to explore this option.

6.2 Modification of v_s

The second step involves the substitution of a new expression for v_s representing the effect of horizontal reinforcement on strength. It has been frequently suggested that horizontal bars provide post cracking resistance in direct tension [11,12]. A commonly suggested model for this effect is the expression

$$v_s = k.\rho_h.f_{yh},$$

where k is a numerical constant. This expression is adopted for v_s in Equation (6) except ρ_h is raised to the power of 0.31 to account for the decreasing influence of increasing horizontal reinforcement on strength (as observed in the present study). The factors γ and δ in the original equation are retained. The numerical values of the coefficient and exponent to ρ_v have been determined by calibration against test results.

6.3 Modification of v_q

The last functional change is made in the contribution of v_q to predicted strength. To account for the presence of a residual post-cracking masonry strength in the absence of axial load, a new term proportional to the compressive strength of masonry is added. The residual post-cracking masonry strength in the absence of axial load is attributed to the resistance of the compression zone near the loaded corner and the corner diagonally opposite to it. This resistance is sometimes referred to as aggregate interlock [12]. The numerical constants in the functions for f_m and q have been evaluated by calibration against selected test results in the same manner as noted above.

6.4 Comparison of Predictive Equations

Figure 14 displays the data points of the strength ratios (v_p/v_t) in which v_p is calculated by Equation (1) and v_t is the measured strength of the 72 PG specimens examined in this study. It shows that predicted strength varies from 23% to 180% of measured strength. The predicted strength of 39 specimens (54% of the total) exceeded the range of ±20% of test strength (i.e., v_p/v_t = 0.80 to 1.20). This comparison shows a deviation of 0.25 MPa (36 psi), which is about one-third (v_a = 0.31) of the average test strength of 0.79 MPa (115 psi). The figure highlights the very low strength estimates for unreinforced walls (Nos. 52, 56 and 63), and for walls in which no vertical bars were used (Nos. 64-72). By contrast, the strength of most concrete block walls of data set M are overestimated.

Figure 15 is similar to Figure 14 except Equation (6) is used to calculate predicted strength, v_p. It shows considerable improvement in the accuracy of the predictions. The range of scatter of the strength ratios is narrowed to 41-146%, with 68% (50 out of 72 tests) falling within ±20% of measured strength. The deviation and variation have decreased from 0.25 to 0.17 MPa (30 to 25 psi), and from 0.31 to 0.21, respectively.

In an earlier study [2], the ability of equation (1) to predict the strength of fully-grouted walls was examined by checking it against the test results of 62 specimens. Figure 16 plots the strength ratios v_p/v_t for these fully-grouted specimens. Predicted strength

varied from 53% to 160% of measured strength with the ratios of 16 specimens falling outside the ±20% range. The average strength of the 62 tests was 2.10 MPa (305 psi). The deviation and variation were 0.43 MPa (62 psi) and 0.21, respectively.

Figure 17 is similar to Figure 16 except Equation (6) was used to calculate v_p. Predicted strengths vary from 47% to 128% of the corresponding measurements with the strength ratio of 11 specimens falling outside the ±20% range. The deviation and variation are .39 MPa (56 psi) and 0.19, respectively. While the predictions based on Equation (6) are closer to the measurements than those based on Equation (1), the improvement is not as substantial as for the partially-grouted walls because the original predictions for the fully-grouted walls showed less scatter than those for the partially-grouted specimens.

Equation (6) is a step toward developing a rational basis for the analysis of masonry shear wall strength. To reach this goal will require additional tests of partially-grouted masonry shear walls, coupled with studies of the interaction of critical parameters, the relationship between bearing strength of grout and the compressive strength of grouted masonry prisms, and the effect of differences in the compressive strengths of concrete block and brick masonry.

6.5 Summary

This Section presented a methodology which can be used to derive equations for the prediction of the strength of masonry shear walls using experimental measurements and suggested models of post-cracking behavior. It should be noted that the bulk of the experimental data, data set M (51 of a total 72 tests), came from the researcher who proposed the predictive equation (Equation 1) examined in this study. Since the equation was developed through calibration mostly against data set M, the accuracy of the improved predictive function (Equation 6) should be tested against additional measurements. At present, not many partially-grouted shear wall tests are available from U.S. sources other than the 21 tests examined in this study. This number of tests is not sufficient to validate the ability of Equation (1) to predict masonry shear wall strength. On the other hand, the moderate improvement in correlation of strength predictions based on equation (6) with the test results of 62 fully-grouted walls assembled from four independent experimental sources [2] is significant.

7. SUMMARY AND CONCLUSIONS

A proposed equation (Equation 1) developed by Matsumura for the prediction of the shear strength of partially-grouted masonry shear

walls was evaluated against the test results of 72 specimens obtained from three independent research sources. Fifty one specimens were tested in Japan and reported by Matsumura (data set M); eleven at the University of California, Berkeley (data set B); and ten at NIST (data set N). To improve the correlation, a modified equation was developed (Equation 6) by changing the functional forms of the parametric effects in Equation (1) to reflect more closely post-cracking resistance mechanisms of masonry shear walls, and was evaluated against the same test results. The following observations and conclusions are drawn from the study.

1. The correlation of Equation (1) with the test results of data set M is close for high strength specimens (Figure 2b), most of which were of clay brick construction. Generally, as measured strength decreases, the correlation becomes weaker and scatter increases (Figure 2a).

2. Equation (1) makes no provision for considering the effect of the compressive strength of masonry on the shear strength of unreinforced walls which carry no axial load ($v_p = 0$).

3. Equation (1) predicted the measured strengths of the six reinforced concrete block specimens of aspect ratio of 1.2 of data set B reasonably well, but the correlation with the measured strengths of the three clay brick specimens of aspect ratio of 1.9 was weak. Equation (1) could not predict the strengths of the two unreinforced walls of data set B.

4. Equation (1) showed an almost complete lack of correlation with the test results of the nine horizontally-reinforced specimens and the one unreinforced specimen of data set N.

5. The validity of some of the functional forms of the parameters used in the predictive equation in simulating shear wall behavior is questioned.

6. Based on the 72 tests studied, Equation (1) predicted strengths which varied from a low of 23% of measured strength for a unreinforced wall, to a high of 180% of measured strength for a concrete block wall reinforced horizontally and vertically. Less than half of the predicted strengths were within ±20% of the measured strengths.

7. Equation (6) showed substantially closer correlation with the test results than equation (1). Predicted strength varied from 41% to 146% of measured strength, 68% of the predicted strengths falling within ±20% of measured strength. Equation (6) was also in better agreement than Equation (1) with the measured strengths of 62 fully-grouted specimens examined in an earlier study.

8. The modified equation is viewed as a first step. Additional tests will be needed to refine the functional forms of the parametric effects in Equation (6) and test them for consistency through comparison with new test data.

8. REFERENCES

1. Yancey, C.W.C., Fattal, S.G., and Dikkers, R.D., Review of Technical Literature on Masonry Shear Walls, NISTIR 90-4512, National Institute of Standards and Technology, Gaithersburg, MD, December, 1990.

2. Fattal, S.G., and Todd D.R., Ultimate Strength of Masonry Shear Walls: Predictions vs Test Results, NISTIR 91-4633, National Institute of Standards and Technology, Gaithersburg, MD, November, 1991.

3. Matsumura Akira, Shear Strength of Reinforced Hollow Unit Masonry Walls, Second Meeting of the U.S.-Japan Joint Technical Coordinating Committee on Masonry Research, Keystone, Colorado, September, 1986.

4. Matsumura Akira, Shear Strength of Reinforced Hollow Units Masonry Walls, Proceedings, Fourth North American Masonry Conference, Paper No. 50, Los Angeles, California, 1987.

5. Chen Shy-Wen J., Hidalgo Pedro A., Mayes Ronald L., Clough Ray W., and McNiven Hugh D., Cyclic Loading Tests of Masonry Single Piers, Volume 2 - Height to Width Ratio of 1, Report No. UCB/EERC-78/28, University of California, Berkeley, California, December, 1978.

6. Hidalgo Pedro A., Mayes Ronald L., McNiven Hugh D., and Clough Ray W., Cyclic Loading Tests of Masonry Single Piers, Volume 1 - Height to Width Ratio of 2, Report No. UCB/EERC-78/27, University of California, Berkeley, California, November, 1978.

7. Yancey C.W.C., and Scribner, C.F., Influence of Horizontal Reinforcement on Shear Resistance of Concrete Block Masonry Walls, NISTIR 89-4202, National Institute of Standards and Technology, Gaithersburg, MD, November, 1989.

8. Blume John A., and Proulx Jacques, Shear in Grouted Brick Masonry Wall Elements, Western States Clay Products Association, San Francisco, California, August, 1968.

9. Jolley R. H., Shear Strength: A predictive Technique for Masonry Walls, PhD Dissertation, Brigham Young University, Provo, Utah, April, 1976.

10. Yokel Felix Y., and Fattal S. George, A Failure Hypothesis for Masonry Shear Walls, NBSIR 75-703, National Bureau of Standards, Gaithersburg, Maryland, May, 1975.

11. Shing P. B., Schuller M., Hoskere V.S., and Carter E., Flexural and Shear Response of Reinforced Masonry Walls, ACI Structural Journal, V. 87, No. 6, November-December, 1990.

12. Priestley M.J.N., and Bridgeman D.O., Seismic Resistance of Brick Masonry Walls, Bulletin of the New Zealand National Society for Earthquake Engineering, Vol. 7, No. 4, December, 1974.

Table 1. Properties of partially-grouted specimens

SPECIMEN I.D.	TEST NO.	h (mm)	L (mm)	t (mm)	d (mm)	sh (mm)	fyh (MPa)	fyve (MPa)	fyvi (MPa)
CW411-M	1	1800	1720	150	1655	0	385.56	385.56	385.56
CW412-M	2	1800	1720	150	1655	0	385.56	385.56	385.56
CW311-M	3	1800	1320	150	1255	0	385.56	385.56	385.56
CW312-M	4	1800	1320	150	1255	0	385.56	385.56	385.56
CW211-M	5	1800	920	150	855	0	385.56	385.56	385.56
CW212-M	6	1800	920	150	855	0	385.56	385.56	385.56
CW301-M	7	1800	1320	150	1255	0	385.56	385.56	385.56
CW302-M	8	1800	1320	150	1255	0	385.56	385.56	385.56
CW31P-M	9	1800	1320	150	1255	0	385.56	385.56	385.56
CW32-M	10	1800	1320	150	1255	0	385.56	385.56	385.56
CW33-M	11	1800	1320	150	1255	0	385.56	385.56	385.56
CW31A2-M	12	1800	1320	150	1255	0	385.56	385.56	385.56
CW31A3-M	13	1800	1320	150	1255	0	385.56	385.56	385.56
CW31A4-M	14	1800	1320	150	1255	0	385.56	385.56	385.56
CW30A2-M	15	1800	1370	150	1293	0	385.56	385.56	385.56
CW32A2-M	16	1800	1370	150	1293	0	385.56	385.56	385.56
CW33A2-M	17	1800	1370	150	1293	0	385.56	385.56	385.56
CW34A2-M	18	1800	1370	150	1293	0	385.56	385.56	385.56
CWB31PA2-	19	1800	1370	150	1293	0	385.56	385.56	385.56
CW30A3-M	20	1800	1320	150	1255	0	385.56	385.56	385.56
CW30PA3-M	21	1800	1320	150	1255	0	385.56	385.56	385.56
CW32A3-M	22	1800	1320	150	1255	0	385.56	385.56	385.56
CW33A3-M	23	1800	1320	150	1255	0	385.56	385.56	385.56
CW52PA21-	24	1800	1970	150	1880	0	385.56	385.56	385.56
CW52PA22-	25	1800	1970	150	1880	0	385.56	385.56	385.56
CW42PA2-M	26	1800	1770	150	1680	0	385.56	385.56	385.56
CW32PA2-M	27	1800	1370	150	1280	0	385.56	385.56	385.56
CW22PA21-	28	1800	970	150	880	0	385.56	385.56	385.56
CW22PA22-	29	1800	970	150	880	0	385.56	385.56	385.56
CNS301-M	30	590	520	150	455	0	385.56	385.56	385.56
CNS302-M	31	590	520	150	455	0	385.56	385.56	385.56
CNS601-M	32	1190	520	150	455	0	385.56	385.56	385.56
CNS602-M	33	1190	520	150	455	0	385.56	385.56	385.56
CNS611-M	34	1190	520	150	455	0	385.56	385.56	385.56
CNS612-M	35	1190	520	150	455	0	385.56	385.56	385.56
CNS901-M	36	1790	520	150	455	0	385.56	385.56	385.56
CNS902-M	37	1790	520	150	455	0	385.56	385.56	385.56
CNS911-M	38	1790	520	150	455	0	385.56	385.56	385.56
CNS912-M	39	1790	520	150	455	0	385.56	385.56	385.56
WS4-M	40	1600	1320	150	1255	0	385.56	385.56	385.56
WS4B-M	41	1600	1320	150	1255	0	385.56	385.56	385.56
WS20-M	42	1600	720	150	655	0	385.56	385.56	385.56
WS21-M	43	1600	720	150	655	0	385.56	385.56	385.56
WS22-M	44	1600	720	150	655	0	385.56	385.56	385.56
WS23-M	45	1600	720	150	655	0	385.56	385.56	385.56
NS31-M	46	300	400	150	345	0	385.56	385.56	385.56
NS32-M	47	300	400	150	345	0	385.56	385.56	385.56
NS61-M	48	600	400	150	345	0	385.56	385.56	385.56
NS62-M	49	600	400	150	345	0	385.56	385.56	385.56
NS91-M	50	900	400	150	345	0	385.56	385.56	385.56
NS92-M	51	900	400	150	345	0	385.56	385.56	385.56
BL2P-B	52	1422.4	1219.2	193.675	1066.8	0	0.00	0.00	0.00
BL5P-B	53	1422.4	1219.2	193.675	1066.8	1422.4	330.58	488.59	0.00
BL8P-B	54	1422.4	1219.2	193.675	1066.8	0	0.00	0.00	0.00
BL10P-B	55	1422.4	1219.2	193.675	1066.8	711.2	330.58	477.48	0.00
BR2P-B	56	1422.4	1219.2	187.325	1066.8	0	0.00	0.00	0.00
BR5P-B	57	1422.4	1219.2	187.325	1066.8	1422.4	483.00	492.25	0.00
BR9P-B	58	1422.4	1219.2	187.325	1066.8	0	0.00	0.00	0.00
BR11P-B	59	1422.4	1219.2	187.325	1066.8	711.2	474.10	502.80	0.00
BR3P1-B	60	2032	1066.8	187.325	914.4	0	342.93	326.37	326.37
BR5P1-B	61	2032	1066.8	187.325	914.4	677.3333	342.93	326.37	326.37
BR7P1-B	62	2032	1066.8	187.325	914.4	508	342.93	326.37	326.37
R1-N	63	1422.4	1219.2	193.675	1066.8	0	0.00	0.00	0.00
R2-N	64	1422.4	1219.2	193.675	1066.8	0	276.00	0.00	0.00
R4-N	65	1422.4	1219.2	193.675	1066.8	0	276.00	0.00	0.00
R5-N	66	1422.4	1219.2	193.675	1066.8	0	336.38	0.00	0.00
R6-N	67	1422.4	1219.2	193.675	1066.8	0	370.07	0.00	0.00
R7-N	68	1422.4	1219.2	193.675	1066.8	0	385.02	0.00	0.00
R8-N	69	1422.4	1219.2	193.675	1066.8	0	373.81	0.00	0.00
R9-N	70	1422.4	1219.2	193.675	1066.8	0	303.60	0.00	0.00
R10-N	71	1422.4	1219.2	193.675	1066.8	0	341.55	0.00	0.00
R11-N	72	1422.4	1219.2	193.675	1066.8	0	372.95	0.00	0.00

Table 1. (Cont.)

TEST NO.	fyv (MPa)	pve	pvi (Avi/tL)	pv	ph	r	rd	q (MPa)	f m (MPa)
1	385.56	0.00300	0.000825		0.00071	1.05	1.09	0	9.51
2	385.56	0.00370	0.000825		0.00071	1.05	1.09	0	15.62
3	385.56	0.00391	0.000716		0.00071	1.36	1.43	0	9.51
4	385.56	0.00357	0.000716		0.00071	1.36	1.43	0	15.62
5	385.56	0.00561	0.001028		0.00071	1.96	2.11	0	9.51
6	385.56	0.00367	0.001028		0.00071	1.96	2.11	0	15.62
7	385.56	0.00391	0.000716		0	1.36	1.43	0	9.51
8	385.56	0.00391	0.000716		0	1.36	1.43	0	9.51
9	385.56	0.00391	0.000716		0.00071	1.36	1.43	0	9.51
10	385.56	0.00391	0.000716		0.00148	1.36	1.43	0	9.51
11	385.56	0.00391	0.000716		0.00222	1.36	1.43	0	9.51
12	385.56	0.00391	0.000716		0.00071	1.36	1.43	0.490711	15.62
13	385.56	0.00391	0.000716		0.00071	1.36	1.43	0.981422	15.62
14	385.56	0.00391	0.000716		0.00071	1.36	1.43	1.472133	15.62
15	385.56	0.00377	0.000690		0	1.31	1.39	0.490711	8.11
16	385.56	0.00377	0.000690		0.00148	1.31	1.39	0.490711	8.11
17	385.56	0.00377	0.000690		0.00222	1.31	1.39	0.490711	8.11
18	385.56	0.00377	0.000690		0.00335	1.31	1.39	0.490711	8.11
19	385.56	0.00140	0.000690		0.00071	1.31	1.39	0.490711	8.11
20	385.56	0.00391	0.000716		0	1.36	1.43	0.981422	15.62
21	385.56	0.00391	0.000716		0	1.36	1.43	0.981422	8.11
22	385.56	0.00391	0.000716		0.00148	1.36	1.43	0.981422	15.62
23	385.56	0.00391	0.000716		0.00222	1.36	1.43	0.981422	15.62
24	385.56	0.00261	0.000960		0.00148	0.91	0.96	0.490711	8.81
25	385.56	0.00261	0.000960		0.00148	0.91	0.96	0.490711	8.81
26	385.56	0.00242	0.000801		0.00148	1.02	1.07	0.490711	8.81
27	385.56	0.00247	0.000690		0.00148	1.31	1.41	0.490711	8.81
28	385.56	0.00266	0.000487		0.00148	1.86	2.05	0.490711	8.81
29	385.56	0.00266	0.000487		0.00148	1.86	2.05	0.490711	8.81
30	385.56	0.01018	0		0	1.13	1.30	0	9.51
31	385.56	0.01018	0		0	1.13	1.30	0	9.61
32	385.56	0.01018	0		0	2.29	2.62	0	9.51
33	385.56	0.01018	0		0	2.29	2.62	0	9.61
34	385.56	0.01018	0		0.00071	2.29	2.62	0	9.51
35	385.56	0.01018	0		0.00071	2.29	2.62	0	9.61
36	385.56	0.01018	0		0	3.44	3.93	0	9.51
37	385.56	0.01018	0		0	3.44	3.93	0	9.61
38	385.56	0.01018	0		0.00071	3.44	3.93	0	9.51
39	385.56	0.01018	0		0.00071	3.44	3.93	0	9.51
40	385.56	0.00391	0.000716		0.00107	1.21	1.27	0	16.22
41	385.56	0.00391	0.000716		0.00107	1.21	1.27	0	17.63
42	385.56	0.00717	0.000657		0	2.22	2.44	0	16.22
43	385.56	0.00717	0.000657		0.00107	2.22	2.44	0	16.22
44	385.56	0.00717	0.000657		0.00222	2.22	2.44	0	16.22
45	385.56	0.00717	0.000657		0.00335	2.22	2.44	0	16.22
46	385.56	0.00845	0		0.00107	0.75	0.87	0	19.13
47	385.56	0.00845	0		0.00107	0.75	0.87	0	24.54
48	385.56	0.00845	0		0.00107	1.50	1.74	0	19.13
49	385.56	0.00845	0		0.00107	1.50	1.74	0	24.54
50	385.56	0.00845	0		0.00107	2.25	2.61	0	19.13
51	385.56	0.00845	0		0.00107	2.25	2.61	0	30.24
52	0.00	0.00000	0	0	0	1.17	1.33	0.7935	9.18
53	488.59	0.00085	0	0.001693	0.000725	1.17	1.33	0.5727	12.65
54	0.00	0.00216	0	0.004316	0	1.17	1.33	0.552	13.14
55	477.48	0.00216	0	0.004316	0.001451	1.17	1.33	0.5865	13.14
56	0.00	0.00000	0	0	0	1.17	1.33	1.4904	17.49
57	492.25	0.00088	0	0.001751	0.000750	1.17	1.33	1.0488	18.78
58	0.00	0.00223	0	0.004463	0	1.17	1.33	0.7245	19.78
59	502.80	0.00223	0	0.004463	0.001501	1.17	1.33	0.5175	18.78
60	326.37	0.00255	0	0.005100	0	1.90	2.22	0.7383	31.06
61	326.37	0.00255	0	0.005100	0.001576	1.90	2.22	1.1937	31.06
62	326.37	0.00255	0	0.005100	0.002101	1.90	2.22	1.1661	31.06
63	0.00	0.00000	0	0	0	1.17		0.740901	8.92
64	0.00	0.00000	0	0	0.000234	1.17		0.740901	8.48
65	0.00	0.00000	0	0	0.000468	1.17		0.740901	7.67
66	0.00	0.00000	0	0	0.000936	1.17		0.740901	8.40
67	0.00	0.00000	0	0	0.002177	1.17		0.740901	8.72
68	0.00	0.00000	0	0	0.000725	1.17		0.740901	7.50
69	0.00	0.00000	0	0	0.002177	1.17		0.740901	8.57
70	0.00	0.00000	0	0	0.000499	1.17		0.740901	7.56
71	0.00	0.00000	0	0	0.002131	1.17		0.740901	5.91
72	0.00	0.00000	0	0	0.000725	1.17		0.740901	7.38

Table 1(a). Properties of partially-grouted specimens
(U.S. Customary Units)

SPECIMEN I.D.	TEST NO.	h (in.)	L (in.)	t (in.)	d (in.)	sh (in.)	fyh (psi)	fyve (psi)	fyvi (psi)
CW411-M	1	70.87	67.72	5.91	65.16		55878	55878	55878
CW412-M	2	70.87	67.72	5.91	65.16		55878	55878	55878
CW311-M	3	70.87	51.97	5.91	49.41		55878	55878	55878
CW312-M	4	70.87	51.97	5.91	49.41		55878	55878	55878
CW211-M	5	70.87	36.22	5.91	33.66		55878	55878	55878
CW212-M	6	70.87	36.22	5.91	33.66		55878	55878	55878
CW301-M	7	70.87	51.97	5.91	49.41		55878	55878	55878
CW302-M	8	70.87	51.97	5.91	49.41		55878	55878	55878
CW31P-M	9	70.87	51.97	5.91	49.41		55878	55878	55878
CW32-M	10	70.87	51.97	5.91	49.41		55878	55878	55878
CW33-M	11	70.87	51.97	5.91	49.41		55878	55878	55878
CW31A2-M	12	70.87	51.97	5.91	49.41		55878	55878	55878
CW31A3-M	13	70.87	51.97	5.91	49.41		55878	55878	55878
CW31A4-M	14	70.87	51.97	5.91	49.41		55878	55878	55878
CW30A2-M	15	70.87	53.94	5.91	50.91		55878	55878	55878
CW32A2-M	16	70.87	53.94	5.91	50.91		55878	55878	55878
CW33A2-M	17	70.87	53.94	5.91	50.91		55878	55878	55878
CW34A2-M	18	70.87	53.94	5.91	50.91		55878	55878	55878
CWB31PA2-	19	70.87	53.94	5.91	50.91		55878	55878	55878
CW30A3-M	20	70.87	51.97	5.91	49.41		55878	55878	55878
CW30PA3-M	21	70.87	51.97	5.91	49.41		55878	55878	55878
CW32A3-M	22	70.87	51.97	5.91	49.41		55878	55878	55878
CW33A3-M	23	70.87	51.97	5.91	49.41		55878	55878	55878
CW52PA21-	24	70.87	77.56	5.91	74.02		55878	55878	55878
CW52PA22-	25	70.87	77.56	5.91	74.02		55878	55878	55878
CW42PA2-M	26	70.87	69.69	5.91	66.14		55878	55878	55878
CW32PA2-M	27	70.87	53.94	5.91	50.39		55878	55878	55878
CW22PA21-	28	70.87	38.19	5.91	34.65		55878	55878	55878
CW22PA22-	29	70.87	38.19	5.91	34.65		55878	55878	55878
CNS301-M	30	23.23	20.47	5.91	17.91		55878	55878	55878
CNS302-M	31	23.23	20.47	5.91	17.91		55878	55878	55878
CNS601-M	32	46.85	20.47	5.91	17.91		55878	55878	55878
CNS602-M	33	46.85	20.47	5.91	17.91		55878	55878	55878
CNS611-M	34	46.85	20.47	5.91	17.91		55878	55878	55878
CNS612-M	35	46.85	20.47	5.91	17.91		55878	55878	55878
CNS901-M	36	70.47	20.47	5.91	17.91		55878	55878	55878
CNS902-M	37	70.47	20.47	5.91	17.91		55878	55878	55878
CNS911-M	38	70.47	20.47	5.91	17.91		55878	55878	55878
CNS912-M	39	70.47	20.47	5.91	17.91		55878	55878	55878
WS4-M	40	62.99	51.97	5.91	49.41		55878	55878	55878
WS4B-M	41	62.99	51.97	5.91	49.41		55878	55878	55878
WS20-M	42	62.99	28.35	5.91	25.79		55878	55878	55878
WS21-M	43	62.99	28.35	5.91	25.79		55878	55878	55878
WS22-M	44	62.99	28.35	5.91	25.79		55878	55878	55878
WS23-M	45	62.99	28.35	5.91	25.79		55878	55878	55878
NS31-M	46	11.81	15.75	5.91	13.58		55878	55878	55878
NS32-M	47	11.81	15.75	5.91	13.58		55878	55878	55878
NS61-M	48	23.62	15.75	5.91	13.58		55878	55878	55878
NS62-M	49	23.62	15.75	5.91	13.58		55878	55878	55878
NS91-M	50	35.43	15.75	5.91	13.58		55878	55878	55878
NS92-M	51	35.43	15.75	5.91	13.58		55878	55878	55878
BL2P-B	52	56.00	48.00	7.63	42.00				
BL5P-B	53	56.00	48.00	7.63	42.00	56.00	47910	70810	
BL8P-B	54	56.00	48.00	7.63	42.00				
BL10P-B	55	56.00	48.00	7.63	42.00	28.00	47910	69200	
BR2P-B	56	56.00	48.00	7.38	42.00				
BR5P-B	57	56.00	48.00	7.38	42.00	56.00	70000	71340	
BR9P-B	58	56.00	48.00	7.38	42.00				
BR11P-B	59	56.00	48.00	7.38	42.00	28.00	68710	72870	
BR3P1-B	60	80.00	42.00	7.38	36.00		49700	47300	47300
BR5P1-B	61	80.00	42.00	7.38	36.00	26.67	49700	47300	47300
BR7P1-B	62	80.00	42.00	7.38	36.00	20.00	49700	47300	47300
R1-N	63	56.00	48.00	7.63	42.00				
R2-N	64	56.00	48.00	7.63	42.00		40000		
R4-N	65	56.00	48.00	7.63	42.00		40000		
R5-N	66	56.00	48.00	7.63	42.00		48750		
R6-N	67	56.00	48.00	7.63	42.00		53633		
R7-N	68	56.00	48.00	7.63	42.00		55800		
R8-N	69	56.00	48.00	7.63	42.00		54175		
R9-N	70	56.00	48.00	7.63	42.00		44000		
R10-N	71	56.00	48.00	7.63	42.00		49500		
R11-N	72	56.00	48.00	7.63	42.00		54050		

Table 1(a). (Cont.)

TEST NO.	fyv (psi)	pve	pvi (Avi/tL)	pv	ph	r	rd	q (psi)	f m (psi)
1	55878	0.00300	0.00083		0.00071	1.05	1.09	0.00	1379
2	55878	0.00370	0.00083		0.00071	1.05	1.09	0.00	2264
3	55878	0.00391	0.00072		0.00071	1.36	1.43	0.00	1379
4	55878	0.00357	0.00072		0.00071	1.36	1.43	0.00	2264
5	55878	0.00561	0.00103		0.00071	1.96	2.11	0.00	1379
6	55878	0.00367	0.00103		0.00071	1.96	2.11	0.00	2264
7	55878	0.00391	0.00072		0	1.36	1.43	0.00	1379
8	55878	0.00391	0.00072		0	1.36	1.43	0.00	1379
9	55878	0.00391	0.00072		0.00071	1.36	1.43	0.00	1379
10	55878	0.00391	0.00072		0.00148	1.36	1.43	0.00	1379
11	55878	0.00391	0.00072		0.00222	1.36	1.43	0.00	1379
12	55878	0.00391	0.00072		0.00071	1.36	1.43	71.12	2264
13	55878	0.00391	0.00072		0.00071	1.36	1.43	142.24	2264
14	55878	0.00391	0.00072		0.00071	1.36	1.43	213.35	2264
15	55878	0.00377	0.00069		0	1.31	1.39	71.12	1176
16	55878	0.00377	0.00069		0.00148	1.31	1.39	71.12	1176
17	55878	0.00377	0.00069		0.00222	1.31	1.39	71.12	1176
18	55878	0.00377	0.00069		0.00335	1.31	1.39	71.12	1176
19	55878	0.00140	0.00069		0.00071	1.31	1.39	71.12	1176
20	55878	0.00391	0.00072		0	1.36	1.43	142.24	2264
21	55878	0.00391	0.00072		0	1.36	1.43	142.24	1176
22	55878	0.00391	0.00072		0.00148	1.36	1.43	142.24	2264
23	55878	0.00391	0.00072		0.00222	1.36	1.43	142.24	2264
24	55878	0.00261	0.00096		0.00148	0.91	0.96	71.12	1277
25	55878	0.00261	0.00096		0.00148	0.91	0.96	71.12	1277
26	55878	0.00242	0.00080		0.00148	1.02	1.07	71.12	1277
27	55878	0.00247	0.00069		0.00148	1.31	1.41	71.12	1277
28	55878	0.00266	0.00049		0.00148	1.86	2.05	71.12	1277
29	55878	0.00266	0.00049		0.00148	1.86	2.05	71.12	1277
30	55878	0.01018	0.00000		0	1.13	1.30	0.00	1379
31	55878	0.01018	0.00000		0	1.13	1.30	0.00	1393
32	55878	0.01018	0.00000		0	2.29	2.62	0.00	1379
33	55878	0.01018	0.00000		0	2.29	2.62	0.00	1393
34	55878	0.01018	0.00000		0.00071	2.29	2.62	0.00	1379
35	55878	0.01018	0.00000		0.00071	2.29	2.62	0.00	1393
36	55878	0.01018	0.00000		0	3.44	3.93	0.00	1379
37	55878	0.01018	0.00000		0	3.44	3.93	0.00	1393
38	55878	0.01018	0.00000		0.00071	3.44	3.93	0.00	1379
39	55878	0.01018	0.00000		0.00071	3.44	3.93	0.00	1379
40	55878	0.00391	0.00072		0.00107	1.21	1.27	0.00	2351
41	55878	0.00391	0.00072		0.00107	1.21	1.27	0.00	2554
42	55878	0.00717	0.00066		0	2.22	2.44	0.00	2351
43	55878	0.00717	0.00066		0.00107	2.22	2.44	0.00	2351
44	55878	0.00717	0.00066		0.00222	2.22	2.44	0.00	2351
45	55878	0.00717	0.00066		0.00335	2.22	2.44	0.00	2351
46	55878	0.00845	0.00000		0.00107	0.75	0.87	0.00	2772
47	55878	0.00845	0.00000		0.00107	0.75	0.87	0.00	3556
48	55878	0.00845	0.00000		0.00107	1.50	1.74	0.00	2772
49	55878	0.00845	0.00000		0.00107	1.50	1.74	0.00	3556
50	55878	0.00845	0.00000		0.00107	2.25	2.61	0.00	2772
51	55878	0.00845	0.00000		0.00107	2.25	2.61	0.00	4383
52		0.00000	0.00000	0	0	1.17	1.33	115.00	1330
53	70810	0.00085	0.00000	0.001693	0.000725	1.17	1.33	83.00	1833
54		0.00216	0.00000	0.004316	0	1.17	1.33	80.00	1905
55	69200	0.00216	0.00000	0.004316	0.001451	1.17	1.33	85.00	1905
56		0.00000	0.00000	0	0	1.17	1.33	216.00	2535
57	71340	0.00088	0.00000	0.001751	0.000750	1.17	1.33	152.00	2722
58		0.00223	0.00000	0.004463	0	1.17	1.33	105.00	2866
59	72870	0.00223	0.00000	0.004463	0.001501	1.17	1.33	75.00	2722
60	47300	0.00255	0.00000	0.005100	0	1.90	2.22	107.00	4502
61	47300	0.00255	0.00000	0.005100	0.001576	1.90	2.22	173.00	4502
62	47300	0.00255	0.00000	0.005100	0.002101	1.90	2.22	169.00	4502
63		0.00000	0.00000	0	0	1.17		107.38	1293
64		0.00000	0.00000	0	0.000234	1.17		107.38	1230
65		0.00000	0.00000	0	0.000468	1.17		107.38	1112
66		0.00000	0.00000	0	0.000936	1.17		107.38	1217
67		0.00000	0.00000	0	0.002177	1.17		107.38	1263
68		0.00000	0.00000	0	0.000725	1.17		107.38	1087
69		0.00000	0.00000	0	0.002177	1.17		107.38	1242
70		0.00000	0.00000	0	0.000499	1.17		107.38	1095
71		0.00000	0.00000	0	0.002131	1.17		107.38	856
72		0.00000	0.00000	0	0.000725	1.17		107.38	1070

Table 2. Scatter in 9 pairs of of duplicate tests of data set M (S.I. Units)

Pair No.	Test No.	v_t MPa	Averages MPa	Test/Avg. Ratio	% Spread from Avg. MPa
1	3	0.456		1.05	0.032
	9	0.416	0.436	0.95	-0.032
2	7	0.295		0.89	-0.073
	8	0.366	0.330	1.11	0.073
3	30	0.721		0.86	-0.099
	31	0.961	0.841	1.14	0.099
4	32	0.491		1.02	0.014
	33	0.471	0.481	0.98	-0.014
5	34	0.731		1.01	0.005
	35	0.721	0.726	0.99	-0.005
6	36	0.371		0.86	-0.096
	37	0.491	0.431	1.14	0.096
7	38	0.691		1.05	0.037
	39	0.621	0.656	0.95	-0.037
8	24	0.786		1.02	0.011
	25	0.761	0.774	0.98	-0.011
9	28	0.541		1.00	-0.003
	29	0.546	0.543	1.00	0.003
Sum		10.44	5.22	18.00	0.370
Avg		0.580	0.58	1.00	0.041

Table 2(a). Scatter in 9 pairs of of duplicate tests of data set M (U.S. Customary Units)

Pair No.	Test No.	v_t psi	Averages psi	Test/Avg. Ratio	% Spread from Avg. psi
1	3	66.04		1.05	4.60
	9	60.23	63.13	0.95	-4.60
2	7	42.82		0.89	-10.61
	8	52.98	47.90	1.11	10.61
3	30	104.50		0.86	-14.29
	31	139.33	121.92	1.14	14.29
4	32	71.12		1.02	2.08
	33	68.21	69.67	0.98	-2.08
5	34	105.95		1.01	0.69
	35	104.50	105.22	0.99	-0.69
6	36	53.70		0.86	-13.95
	37	71.12	62.41	1.14	13.95
7	38	100.15		1.05	5.34
	39	89.99	95.07	0.95	-5.34
8	24	113.93		1.02	1.62
	25	110.30	112.12	0.98	-1.62
9	28	78.37		1.00	-0.46
	29	79.10	78.74	1.00	0.46
Sum		1512	756	18.00	53.64
Avg		84.02	84.02	1.00	5.96

Table 3. Measured and predicted strengths of P.G. walls

SPECIMEN I.D.	TEST NUMBER	V_m (MPa)	V_a (MPa)	V_q (MPa)	V_p (MPa)	V_t(avg) (MPa)
CW411-M	1	0.587	0.147	0.000	0.734	0.440
CW412-M	2	0.801	0.188	0.000	0.989	0.610
CW311-M	3	0.529	0.145	0.000	0.673	0.455
CW312-M	4	0.659	0.186	0.000	0.845	0.595
CW211-M	5	0.443	0.142	0.000	0.584	0.570
CW212-M	6	0.499	0.181	0.000	0.681	0.530
CW301-M	7	0.529	0.000	0.000	0.529	0.295
CW302-M	8	0.529	0.000	0.000	0.529	0.365
CW31P-M	9	0.529	0.145	0.000	0.673	0.415
CW32-M	10	0.529	0.209	0.000	0.738	0.450
CW33-M	11	0.529	0.256	0.000	0.785	0.560
CW31A2-M	12	0.677	0.186	0.082	0.944	0.690
CW31A3-M	13	0.677	0.186	0.163	1.026	0.720
CW31A4-M	14	0.677	0.186	0.245	1.107	0.905
CW30A2-M	15	0.489	0.000	0.081	0.569	0.470
CW32A2-M	16	0.489	0.192	0.081	0.761	0.740
CW33A2-M	17	0.489	0.235	0.081	0.804	0.840
CW34A2-M	18	0.489	0.288	0.081	0.858	0.950
CWB31PA2-	19	0.363	0.133	0.081	0.576	0.675
CW30A3-M	20	0.677	0.000	0.163	0.840	0.800
CW30PA3-M	21	0.488	0.000	0.163	0.651	0.440
CW32A3-M	22	0.677	0.268	0.163	1.108	0.845
CW33A3-M	23	0.677	0.328	0.163	1.168	0.930
CW52PA21-	24	0.579	0.202	0.082	0.862	0.785
CW52PA22-	25	0.579	0.202	0.082	0.862	0.760
CW42PA2-M	26	0.527	0.201	0.081	0.809	0.740
CW32PA2-M	27	0.441	0.198	0.080	0.719	0.710
CW22PA21-	28	0.339	0.192	0.078	0.609	0.540
CW22PA22-	29	0.339	0.192	0.078	0.609	0.545
CNS301-M	30	0.864	0.000	0.000	0.864	0.720
CNS302-M	31	0.869	0.000	0.000	0.869	0.960
CNS601-M	32	0.531	0.000	0.000	0.531	0.490
CNS602-M	33	0.534	0.000	0.000	0.534	0.470
CNS611-M	34	0.531	0.133	0.000	0.664	0.730
CNS612-M	35	0.534	0.134	0.000	0.668	0.720
CNS901-M	36	0.387	0.000	0.000	0.387	0.370
CNS902-M	37	0.389	0.000	0.000	0.389	0.490
CNS911-M	38	0.387	0.133	0.000	0.521	0.690
CNS912-M	39	0.387	0.133	0.000	0.521	0.620
WS4-M	40	0.930	0.387	0.000	1.317	1.005
WS4B-M	41	0.970	0.403	0.000	1.373	0.940
WS20-M	42	0.854	0.000	0.000	0.854	0.860
WS21-M	43	0.854	0.370	0.000	1.224	1.350
WS22-M	44	0.854	0.533	0.000	1.387	1.600
WS23-M	45	0.854	0.655	0.000	1.509	1.520
NS31-M	46	1.805	0.381	0.000	2.186	2.200
NS32-M	47	2.044	0.432	0.000	2.476	2.360
NS61-M	48	1.177	0.381	0.000	1.558	1.280
NS62-M	49	1.333	0.432	0.000	1.765	1.580
NS91-M	50	0.879	0.381	0.000	1.260	0.980
NS92-M	51	1.106	0.479	0.000	1.585	1.310
BL2P-B	52	0.000	0.000	0.121	0.121	0.475
BL5P-B	53	0.464	0.240	0.088	0.792	0.882
BL8P-B	54	0.627	0.000	0.084	0.711	0.696
BL10P-B	55	0.627	0.346	0.090	1.062	0.916
BR2P-B	56	0.000	0.000	0.228	0.228	0.517
BR5P-B	57	0.457	0.215	0.160	0.833	0.882
BR9P-B	58	0.621	0.000	0.111	0.732	0.834
BR11P-B	59	0.606	0.302	0.079	0.987	0.896
BR3P1-B	60	0.700	0.000	0.111	0.810	0.606
BR5P1-B	61	0.700	0.552	0.179	1.431	1.061
BR7P1-B	62	0.700	0.638	0.175	1.512	1.054
R1-N	63	0.000	0.000	0.113	0.113	0.483
R2-N	64	0.000	0.061	0.113	0.174	0.602
R4-N	65	0.000	0.082	0.113	0.196	0.615
R5-N	66	0.000	0.134	0.113	0.248	0.827
R6-N	67	0.000	0.219	0.113	0.332	0.638
R7-N	68	0.000	0.120	0.113	0.233	0.678
R8-N	69	0.000	0.218	0.113	0.331	0.503
R9-N	70	0.000	0.088	0.113	0.202	0.715
R10-N	71	0.000	0.171	0.113	0.284	0.831
R11-N	72	0.000	0.117	0.113	0.230	0.676
AVERAGES						
SET M:		0.684	0.199	0.040	0.923	0.816
SET B:		0.500	0.208	0.130	0.838	0.802
SET N:		0.000	0.121	0.113	0.234	0.657
TOTAL:		0.561	0.190	0.064	0.815	0.792

Table 3(a). Measured and predicted strengths of P.G. walls
(U. S. Customary Units)

SPECIMEN I.D.	TEST NUMBER	V_m (psi)	V_a (psi)	V_q (psi)	V_p (psi)	V_t(avg) (psi)
CW411-M	1	85.19	21.27	0.00	106.46	63.86
CW412-M	2	116.28	27.25	0.00	143.53	88.53
CW311-M	3	76.72	21.01	0.00	97.73	66.04
CW312-M	4	95.64	26.93	0.00	122.57	86.36
CW211-M	5	64.25	20.54	0.00	84.79	82.73
CW212-M	6	72.49	26.32	0.00	98.81	76.92
CW301-M	7	76.72	0.00	0.00	76.72	42.82
CW302-M	8	76.72	0.00	0.00	76.72	52.98
CW31P-M	9	76.72	21.01	0.00	97.73	60.23
CW32-M	10	76.72	30.34	0.00	107.06	65.31
CW33-M	11	76.72	37.16	0.00	113.87	81.28
CW31A2-M	12	98.31	26.93	11.83	137.07	100.15
CW31A3-M	13	98.31	26.93	23.67	148.90	104.50
CW31A4-M	14	98.31	26.93	35.50	160.73	131.35
CW30A2-M	15	70.90	0.00	11.75	82.65	68.21
CW32A2-M	16	70.90	27.81	11.75	110.46	107.40
CW33A2-M	17	70.90	34.06	11.75	116.71	121.92
CW34A2-M	18	70.90	41.84	11.75	124.49	137.88
CWB31PA2-	19	52.65	19.26	11.75	83.66	97.97
CW30A3-M	20	98.31	0.00	23.67	121.97	116.11
CW30PA3-M	21	70.84	0.00	23.67	94.50	63.86
CW32A3-M	22	98.31	38.88	23.67	160.85	122.64
CW33A3-M	23	98.31	47.62	23.67	169.59	134.98
CW52PA21-	24	83.98	29.31	11.88	125.17	113.93
CW52PA22-	25	83.98	29.31	11.88	125.17	110.30
CW42PA2-M	26	76.50	29.15	11.81	117.46	107.40
CW32PA2-M	27	64.02	28.69	11.63	104.34	103.05
CW22PA21-	28	49.25	27.86	11.29	88.40	78.37
CW22PA22-	29	49.25	27.86	11.29	88.40	79.10
CNS301-M	30	125.45	0.00	0.00	125.45	104.50
CNS302-M	31	126.11	0.00	0.00	126.11	139.33
CNS601-M	32	77.08	0.00	0.00	77.08	71.12
CNS602-M	33	77.48	0.00	0.00	77.48	68.21
CNS611-M	34	77.08	19.34	0.00	96.42	105.95
CNS612-M	35	77.48	19.44	0.00	96.92	104.50
CNS901-M	36	56.23	0.00	0.00	56.23	53.70
CNS902-M	37	56.53	0.00	0.00	56.53	71.12
CNS911-M	38	56.23	19.34	0.00	75.57	100.15
CNS912-M	39	56.23	19.34	0.00	75.57	89.99
WS4-M	40	135.00	56.14	0.00	191.15	145.86
WS4B-M	41	140.71	58.52	0.00	199.24	136.43
WS20-M	42	123.90	0.00	0.00	123.90	124.82
WS21-M	43	123.90	53.72	0.00	177.62	195.94
WS22-M	44	123.90	77.38	0.00	201.28	232.22
WS23-M	45	123.90	95.06	0.00	218.96	220.61
NS31-M	46	261.99	55.30	0.00	317.29	319.30
NS32-M	47	296.72	62.64	0.00	359.36	342.53
NS61-M	48	170.85	55.30	0.00	226.15	185.78
NS62-M	49	193.50	62.64	0.00	256.13	229.32
NS91-M	50	127.61	55.30	0.00	182.92	142.24
NS92-M	51	160.46	69.54	0.00	230.01	190.13
BL2P-B	52	0.00	0.00	17.61	17.61	69.00
BL5P-B	53	67.41	34.80	12.71	114.92	128.00
BL8P-B	54	90.99	0.00	12.25	103.24	101.00
BL10P-B	55	90.99	50.17	13.02	154.17	133.00
BR2P-B	56	0.00	0.00	33.07	33.07	75.00
BR5P-B	57	66.38	31.27	23.28	120.92	128.00
BR9P-B	58	90.18	0.00	16.08	106.26	121.00
BR11P-B	59	87.88	43.81	11.48	143.18	130.00
BR3P1-B	60	101.57	0.00	16.05	117.62	88.00
BR5P1-B	61	101.57	80.17	25.95	207.69	154.00
BR7P1-B	62	101.57	92.58	25.35	219.50	153.00
R1-N	63	0.00	0.00	16.44	16.44	70.09
R2-N	64	0.00	8.87	16.44	25.32	87.43
R4-N	65	0.00	11.94	16.44	28.38	89.21
R5-N	66	0.00	19.49	16.44	35.94	120.08
R6-N	67	0.00	31.76	16.44	48.21	92.62
R7-N	68	0.00	17.35	16.44	33.79	98.36
R8-N	69	0.00	31.66	16.44	48.10	72.95
R9-N	70	0.00	12.83	16.44	29.27	103.83
R10-N	71	0.00	24.85	16.44	41.29	120.63
R11-N	72	0.00	16.94	16.44	33.39	98.09
AVERAGES						
SET M:		99.34	28.89	5.77	134.00	118.43
SET B:		72.59	30.25	18.80	121.65	116.36
SET N:		0.00	17.57	16.44	34.01	95.33
TOTAL:		81.46	27.52	9.24	118.22	114.91

Table 4. Statistical data on predicted vs. measured strength

DATA SET	TEST NO.	EQN.	MAS. TYPE	REGR. CONST C	DEV. S MPa (psi)	MEAN X_m MPa (psi)	VAR. V_a
M	1-39	(1)	CONCR BLOCK	1.134	0.17 (25)	0.63 (92)	0.28
M	40-51	(1)	CLAY BRICK	1.065	0.24 (35)	1.41 (205)	0.17
M	1-51	(1)	COMB	1.091	0.19 (28)	0.81 (118)	0.23
M	1-39	(6)	CONCR BLOCK	———	0.14 (20)	0.63 (92)	0.22
M	40-51	(6)	CLAY BRICK	———	0.20 (29)	1.41 (205)	0.14
M	1-51	(6)	COMB	1.000	0.16 (23)	0.81 (118)	0.19
B	52-62	(1)	ALL	0.746	0.26 (37)	0.80 (116)	0.32
B	53-55 57-62	(1)	REINF	1.146	0.23 (34)	0.87 (126)	0.27
B	53-55 57-59	(1)	REINF	1.004	0.10 (15)	0.86 (124)	0.12
N	63-72	(1)	ALL	0.351	0.46 (67)	0.66 (95)	0.31
N	64-72	(1)	REINF	0.357	0.47 (67)	0.68 (98)	0.70

Table 5. Groupings of data set M tests for comparison of results

Group	Test No.	r	ρ_{ve}	f_m (MPa)	$f_1(r)$	$f_2(\rho_{ve})$	$f_1 . f_2$	v_p/v_t
A	7	1.36	.004	9.52	0.37	5.6	2.07	1.80
	8	1.36	.004	9.52	0.37	5.6	2.07	1.45
B	30	1.13	.010	9.52	0.39	8.6	3.38	1.20
	31	1.13	.010	9.61	0.39	8.6	3.38	0.90
C	32	2.29	.010	9.52	0.24	8.6	2.06	0.85
	33	2.29	.010	9.61	0.24	8.6	2.06	1.14
	36	3.44	.010	9.52	0.18	8.6	1.55	1.04
	37	3.44	.010	9.61	0.18	8.6	1.55	0.80

(9.52 MPa = 1379 psi, 9.61 MPa = 1393 psi)

Table 6. Group of identical tests except in axial stress q.

Group	Test No.	q MPa (psi)	r	f_m MPa (psi)	ρ_{ve}	ρ_h
1	4	0.00 (0.00)	1.36	15.62 (2264)	0.00357	0.00071
	12	0.49 (71.12)	do	do	do	do
	13	0.98 (142.24)	do	do	do	do
	14	1.47 (213.35)	do	do	do	do

Table 7. Six groups of identical tests except in aspect ratio, r.

Group	Test No.	r	f_m MPa (psi)	ρ_{ve}	ρ_h	q MPa (psi)
1	2	1.05	15.62 (2264)	.00370	.00071	0
	4	1.36	do	.00357	do	do
	6	1.96	do	.00367	do	do
2	30,31	1.13	9.52-.61 (1379-93)	.01018	0	0
	32,33	2.29	do	do	do	do
	36,37	3.44	9.61 (1393)	do	do	do
3	34,35	2.29	9.52-.61 (1379-93)	.01018	.00071	0
	38,39	3.44	1379 (9.52)	do	do	do
4	24,25	.914	8.81 (1277)	.00261	.00148	0.49 (71.1)
	26	1.02	do	.00242	do	do
	27	1.31	do	.00247	do	do
	28,29	1.86	do	.00266	do	do
5	46	0.75	19.13 (2772)	.00845	.00107	0
	48	1.50	do	do	do	do
	50	2.25	do	do	do	do
6	47	0.75	24.54 (3556)	.00845	.00107	0
	49	1.50	do	do	do	do
	51	2.25	30.24 (4383)	do	do	do

Table 8. Six groups of identical tests except in ρ_h.

Group	Test No.	ρ_h	f_m MPa (psi)	ρ_{ve}	r	q MPa (psi)
1	7	0	9.52 (1379)	.00391	1.36	0
	8	0	do	do	do	do
	9	.00071	do	do	do	do
	10	.00148	do	do	do	do
	11	.00222	do	do	do	do
2	15	0	8.11 (1176)	.00377	1.31	0.49 (71.1)
	16	.00148	do	do	do	do
	17	.00222	do	do	do	do
	18	.00335	do	do	do	do
3	20	0	15.62 (2264)	.00391	1.36	0.98 (142.2)
	22	.00148	do	do	do	do
	23	.00222	do	do	do	do
4	32,33	0	9.51-.61 (1378-93)	.01018	2.29	0
	34,35	.00071	do	do	do	do
5	36,37	0	9.51-.61 (1378-93)	.01018	3.44	0
	38,39	.00071	9.51 (1378)	do	do	do
6	42	0	16.22 (2351)	.00717	2.22	0
	43	.00107	do	do	do	do
	44	.00222	do	do	do	do
	45	.00335	do	do	do	do

Table 9. Two groups of identical tests except in f_m

Group	Test No.	f_m MPa (psi)	q MPa (psi)	r	ρ_{ve}	ρ_h
1	20	15.62 (2264)	0.98 (142)	1.36	0.00391	0.0
	21	8.11 (1176)	do	do	do	do
2	40	16.22 (2351)	0	1.21	0.00391	0.00107
	41	17.62 (2554)	do	do	do	do

Table 10. Selected data from data sets B and N (S.I. Units)

TEST	r	q	f_m	ρ_{ve}	ρ_h	v_m	v_s	v_q	v_p	v_t
		MPa	MPa			MPa	MPa	MPa	MPa	MPa
BERKELEY TESTS										
52	1.2	0.79	9.18	0	0	0	0	0.12	0.12	0.48
53	1.2	0.57	12.65	.00085	.00072	0.46	0.24	0.09	0.79	0.88
54	1.2	0.55	13.14	.00216	0	0.66	0	0.08	0.71	0.70
55	1.2	0.59	13.14	.00216	.00145	0.66	0.35	0.09	1.06	0.92
56	1.2	1.49	17.49	0	0	0	0	0.23	0.23	0.52
57	1.2	1.05	18.78	.00088	.00075	0.46	0.21	0.16	0.83	0.88
58	1.2	0.72	19.78	.00223	0	0.62	0	0.11	0.73	0.83
59	1.2	0.52	18.78	.00223	.00150	0.61	0.30	0.08	0.99	0.90
60	1.9	0.74	31.06	.00255	0	0.70	0	0.11	0.81	0.61
61	1.9	1.19	31.06	.00255	.00157	0.70	0.55	0.18	1.44	1.06
62	1.9	1.17	31.06	.00255	.00210	0.70	0.64	0.17	1.52	1.06
NIST TESTS										
63	1.2	0.74	8.91	0	0	0	0	0.11	0.11	0.48
64	1.2	0.74	8.49	0	.00023	0	0.06	0.11	0.17	0.60
65	1.2	0.74	7.67	0	.00047	0	0.08	0.11	0.19	0.61
66	1.2	0.74	8.40	0	.00094	0	0.14	0,11	0.25	0.82
67	1.2	0.74	8.71	0	.00218	0	0.22	0.11	0.33	0.63
68	1.2	0.74	7.50	0	.00072	0	0.12	0.11	0.23	0.68
69	1.2	0.74	8.57	0	.00218	0	0.22	0.11	0.33	0.50
70	1.2	0.74	7.56	0	.00050	0	0.09	0.11	0.20	0.71
71	1.2	0.74	5.91	0	.00213	0	0.17	0.11	0.28	0.83
72	1.2	0.74	7.38	0	.00073	0	0.12	0.11	0.22	0.68

Table 10(a). Selected data from data sets B and N (U.S. Customary Units)

TEST	r	q	f_m	ρ_{ve}	ρ_h	v_m	v_s	v_q	v_p	v_t
		psi	psi			psi	psi	psi	psi	psi
BERKELEY TESTS										
52	1.2	115	1330	0	0	0	0	18	18	69
53	1.2	83	1833	.00085	.00072	67	35	13	115	128
54	1.2	80	1905	.00216	0	91	0	12	103	101
55	1.2	85	1905	.00216	.00145	91	50	13	154	133
56	1.2	216	2535	0	0	0	0	33	33	75
57	1.2	152	2722	.00088	.00075	66	31	23	121	128
58	1.2	105	2866	.00223	0	90	0	16	106	121
59	1.2	75	2722	.00223	.00150	88	44	11	143	130
60	1.9	107	4502	.00255	0	102	0	16	118	88
61	1.9	173	4502	.00255	.00157	102	80	26	208	154
62	1.9	169	4502	.00255	.00210	102	93	25	220	153
NIST TESTS										
63	1.2	107	1292	0	0	0	0	16	16	70
64	1.2	107	1230	0	.00023	0	9	16	25	87
65	1.2	107	1112	0	.00047	0	12	16	28	89
66	1.2	107	1217	0	.00094	0	20	16	36	120
67	1.2	107	1263	0	.00218	0	32	16	48	92
68	1.2	107	1087	0	.00072	0	17	16	34	98
69	1.2	107	1242	0	.00218	0	32	16	48	73
70	1.2	107	1095	0	.00050	0	13	16	29	103
71	1.2	107	856	0	.00213	0	25	16	41	121
72	1.2	107	1070	0	.00073	0	17	16	33	98

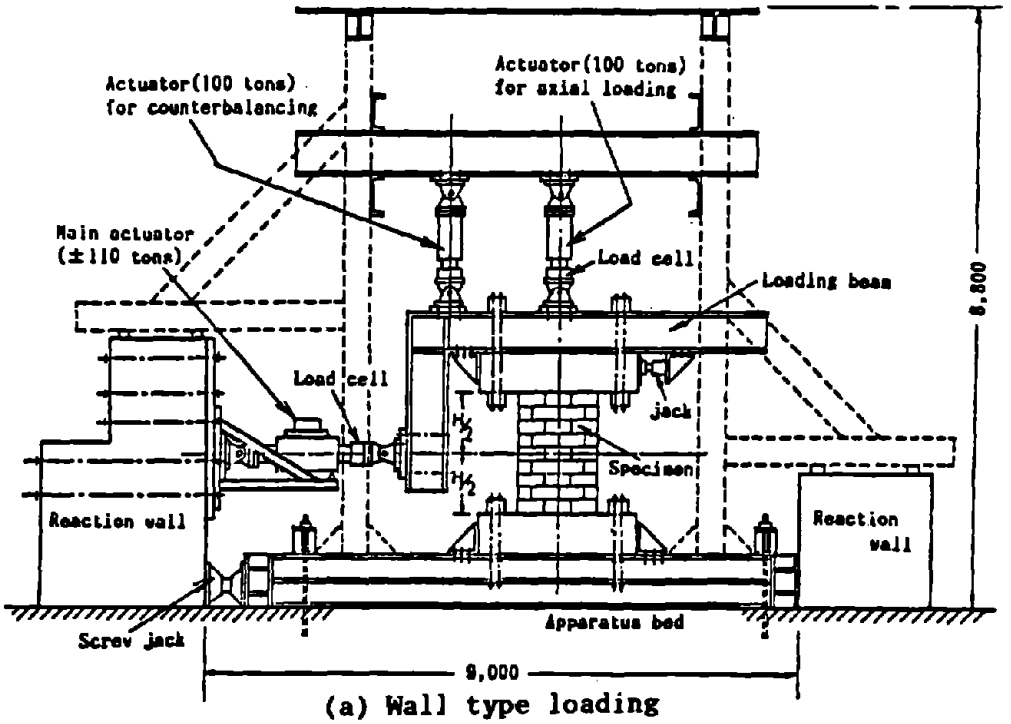

(a) Wall type loading

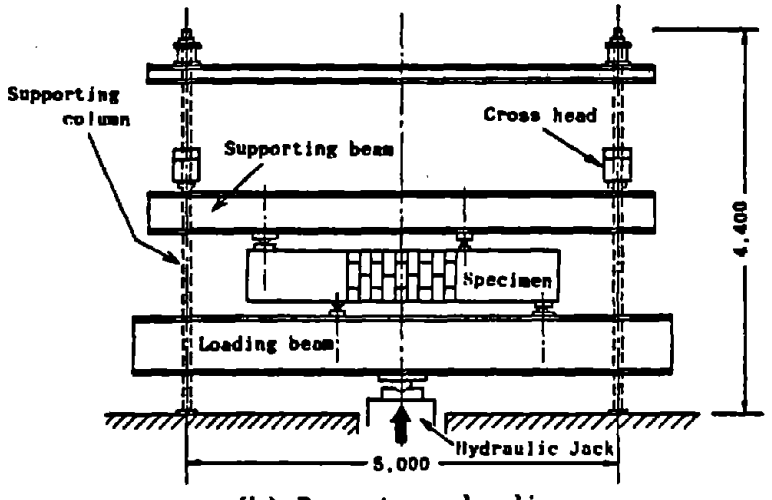

(b) Beam type loading

Figure 1. Outline of loading systems

Figure 2. M-M Comparison

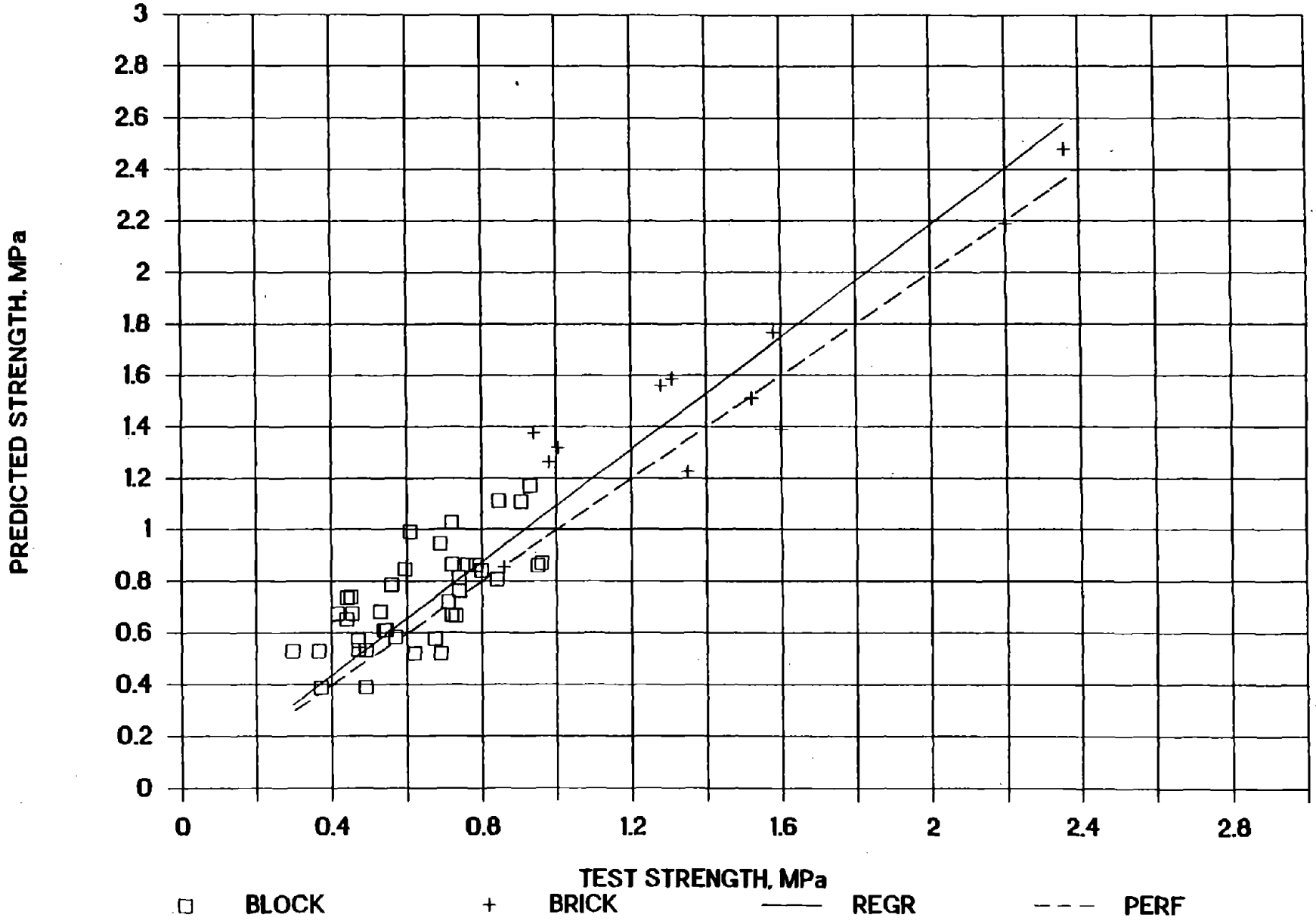

Figure 2a. M-M comparison for CB walls

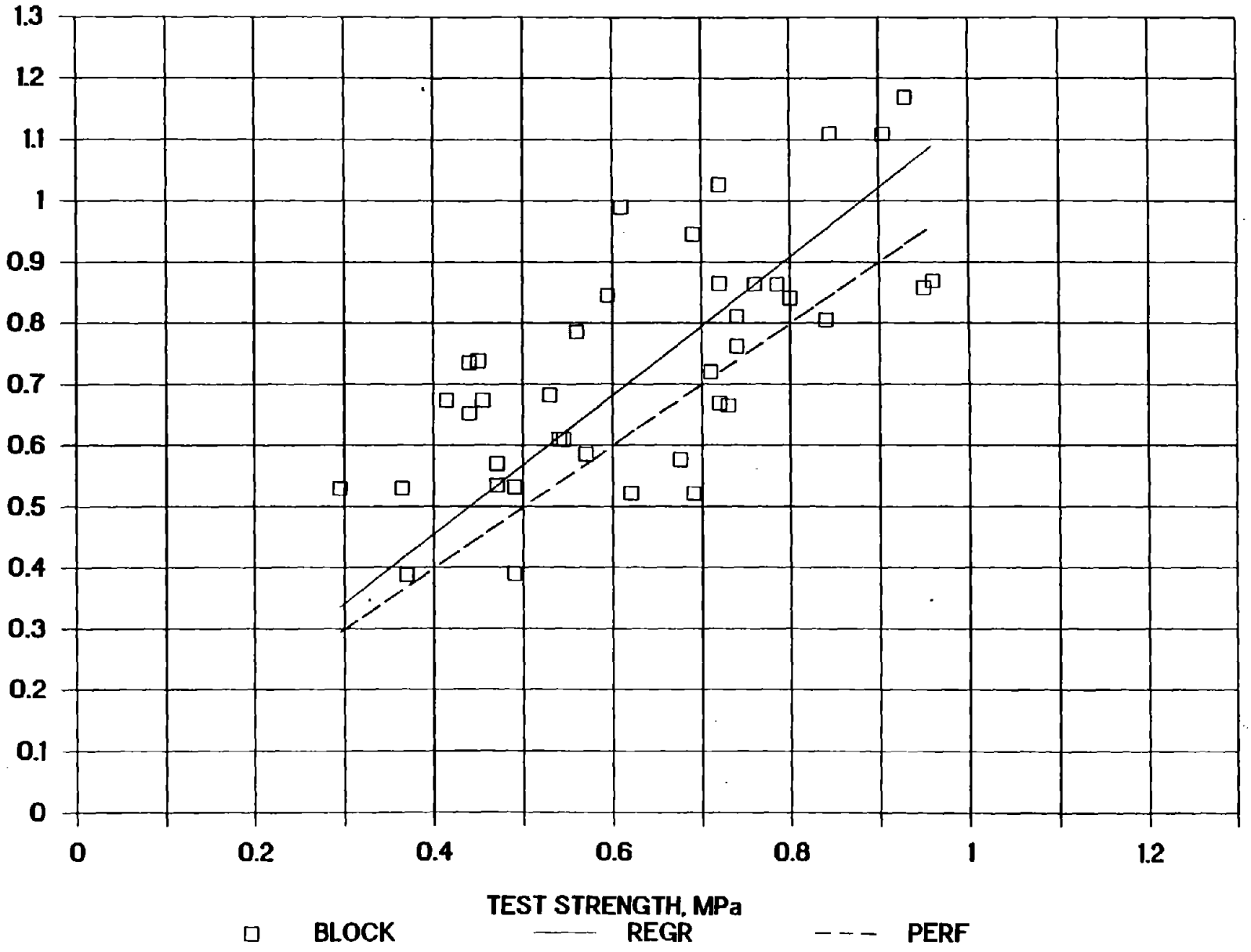

Figure 2b. M-M comparison of BR walls

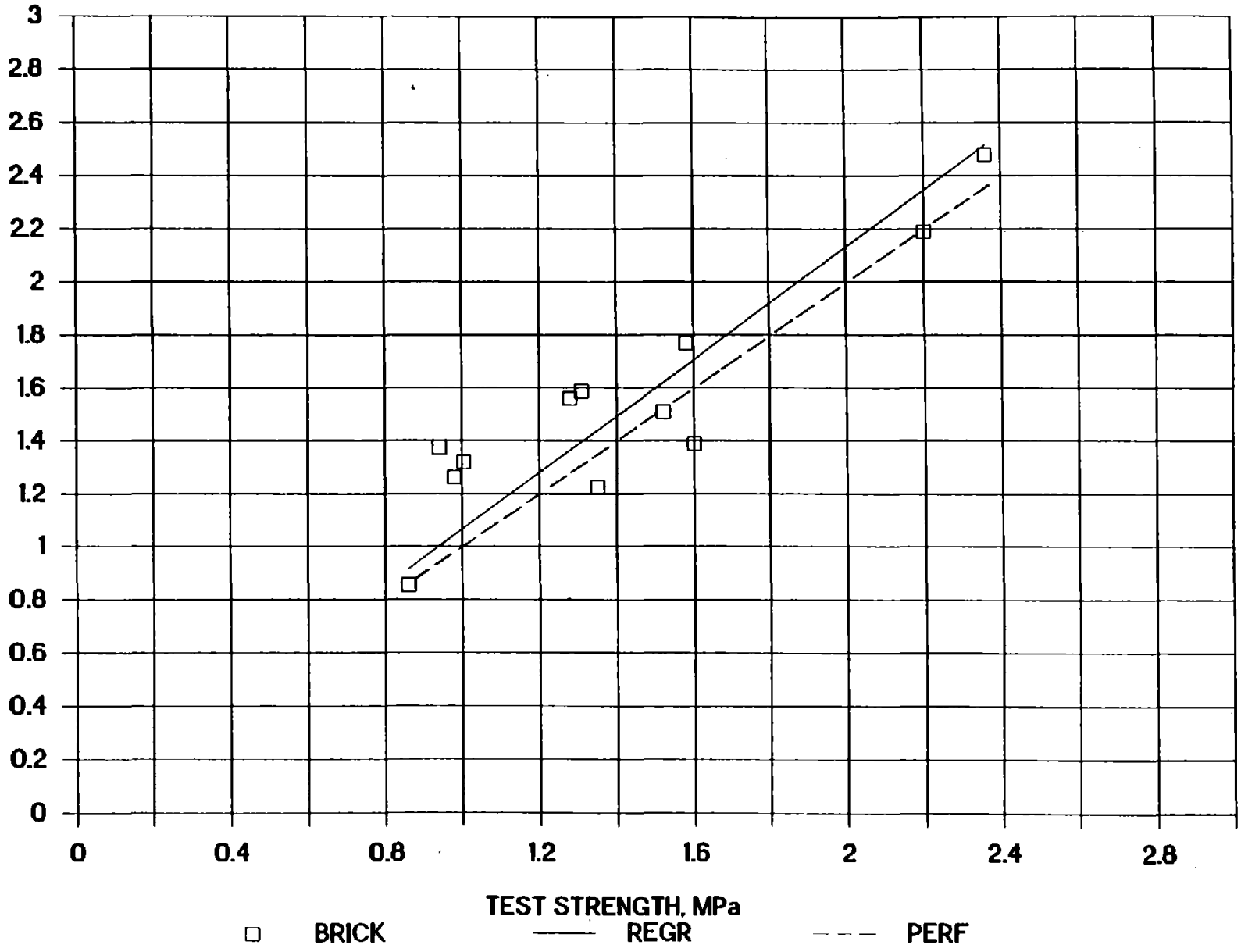

Figure 3. M-B Comparison

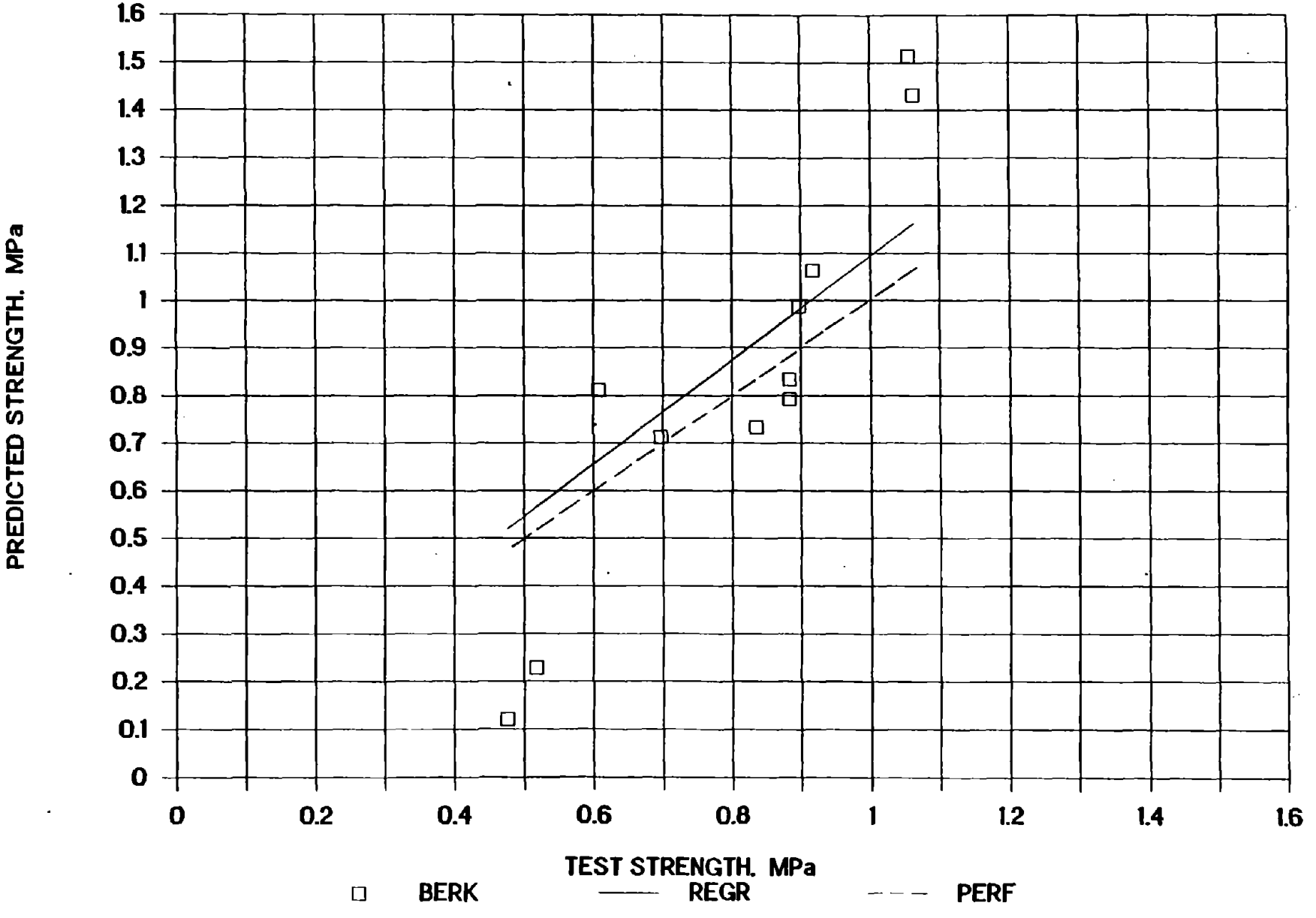

Figure 4. M-N Comparison

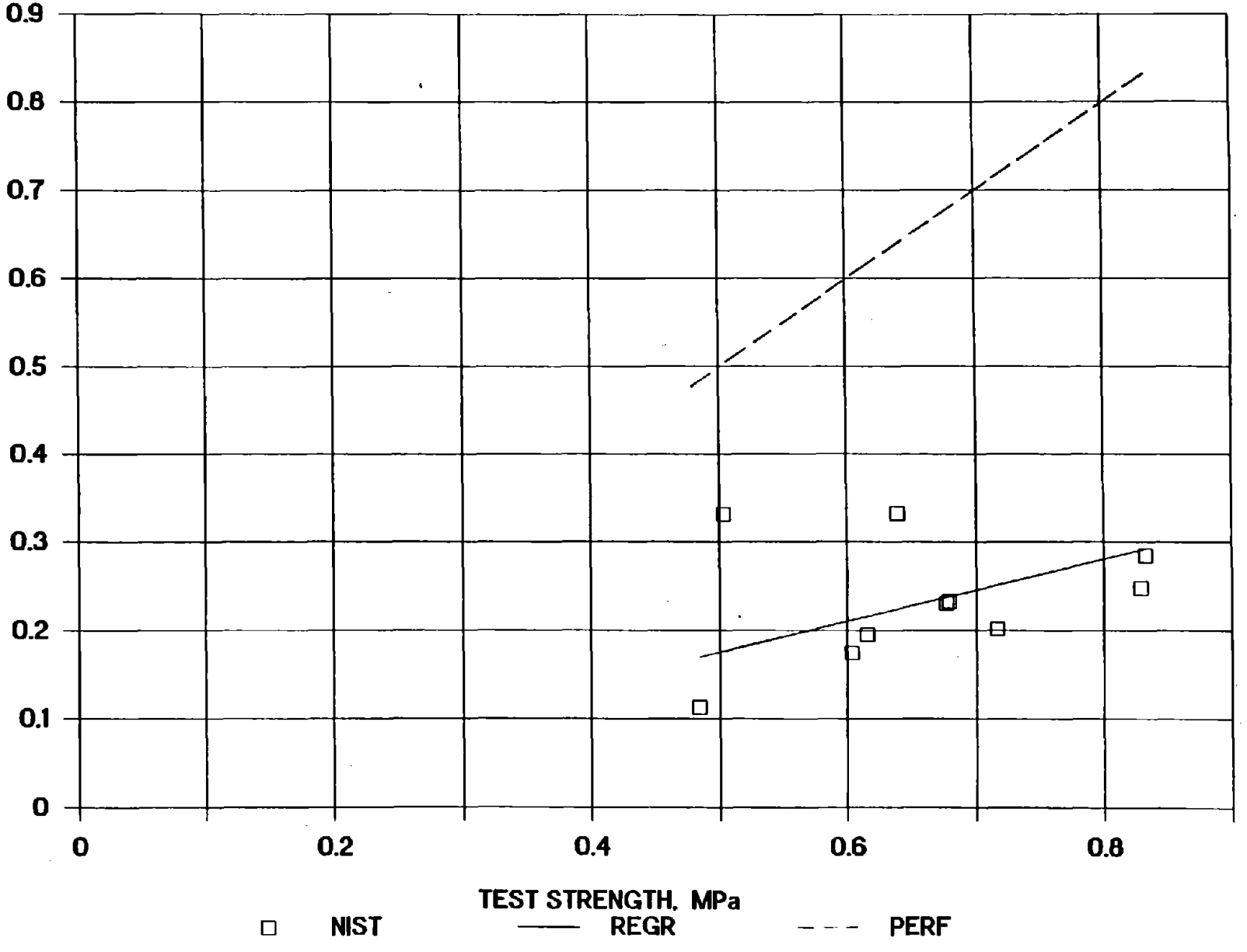

Figure 5. M-T Comparison

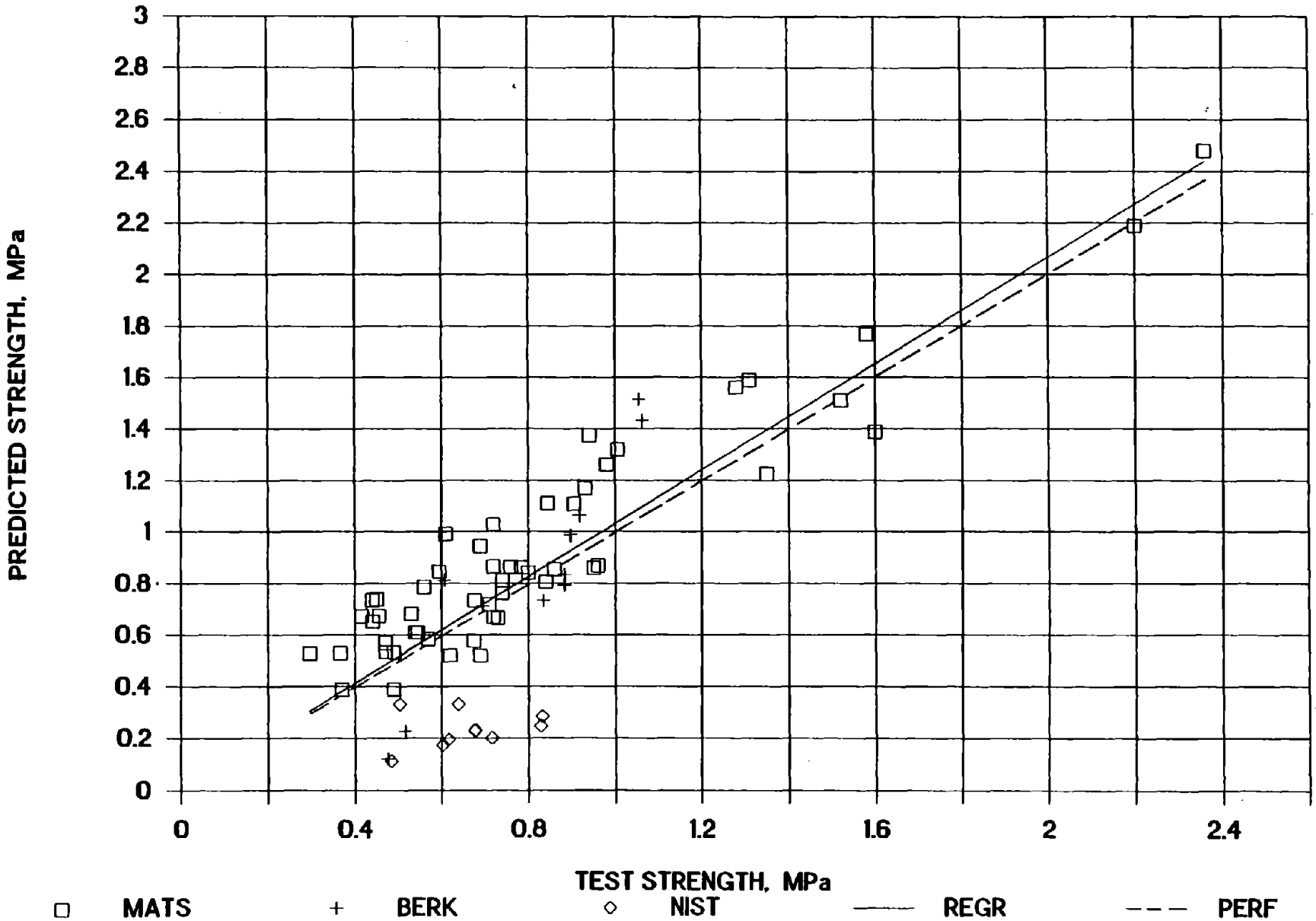

Figure 6. Strength ratios, data set M

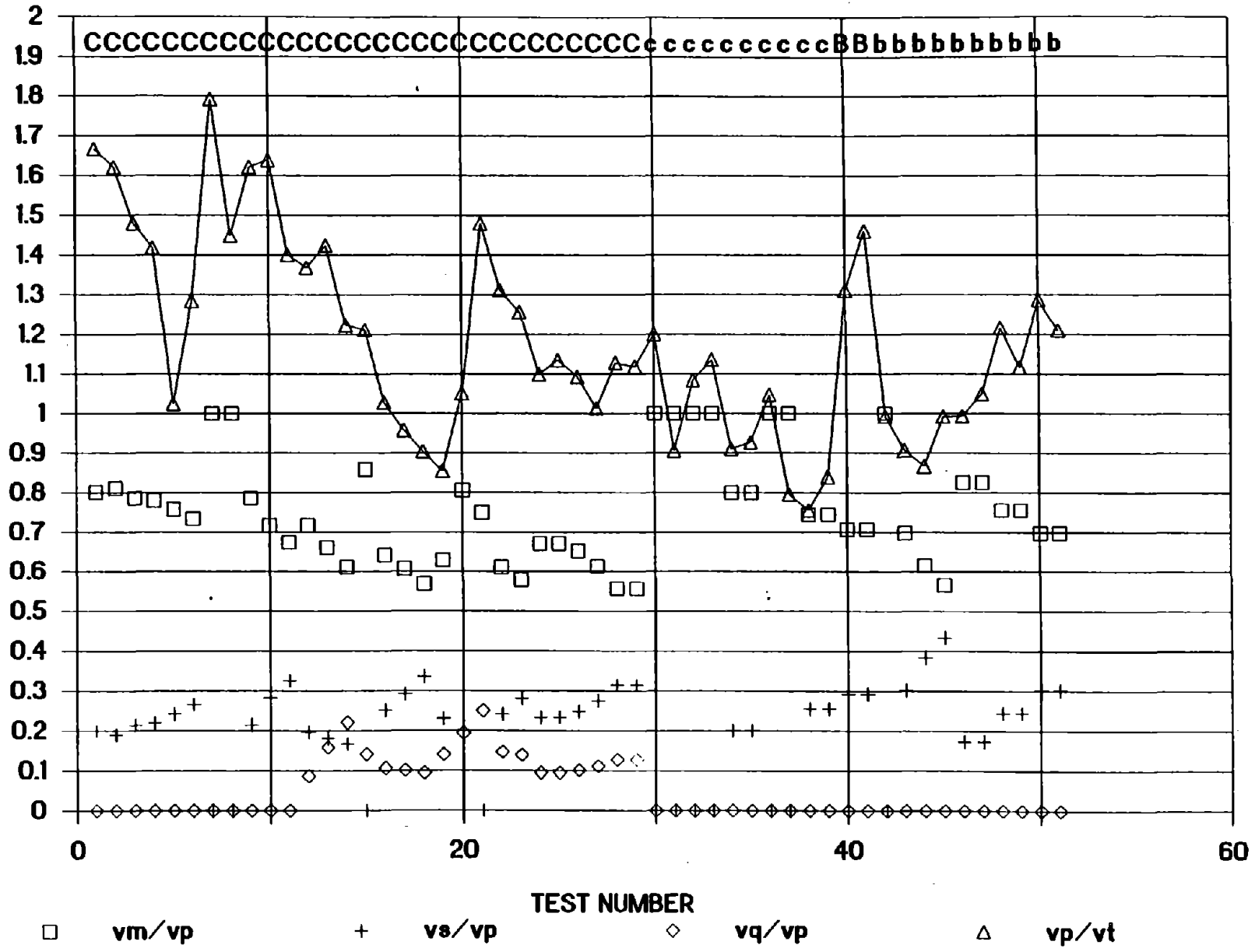

Figure 7. Strength ratios, data set B

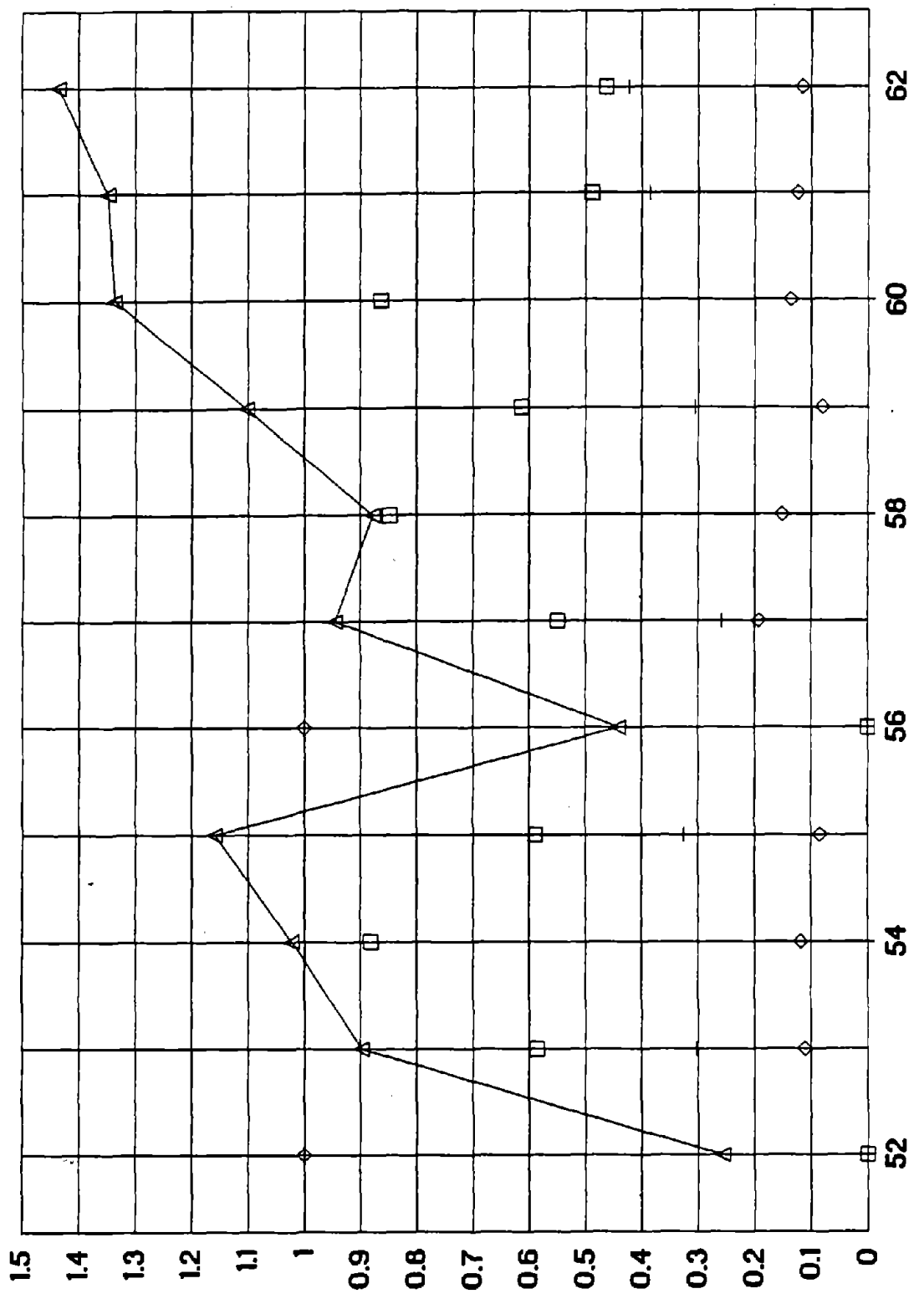

Figure 8. Strength ratios, data set N

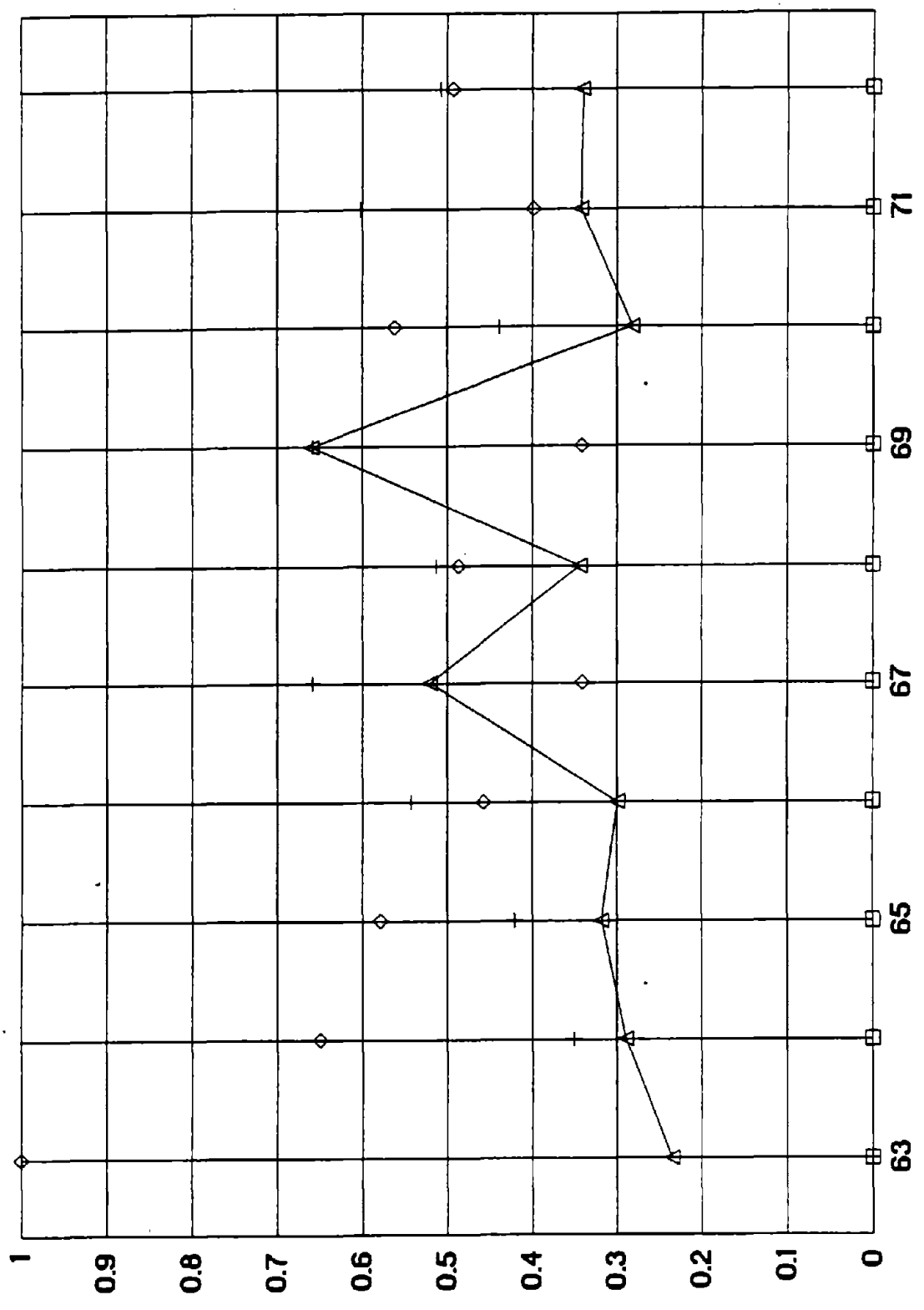

Figure 9. Effect of q on strength

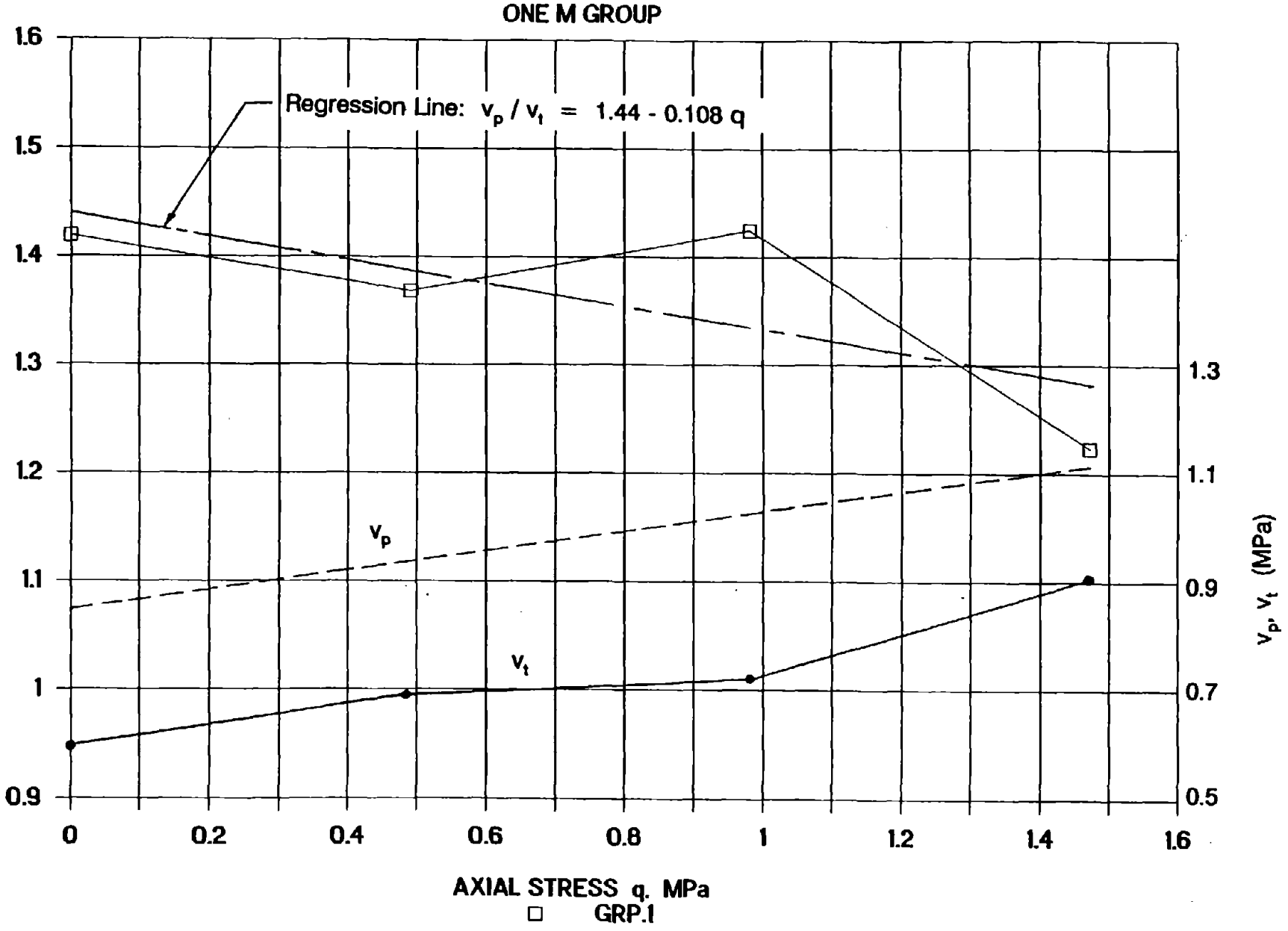

Figure 10. Effect of r on strength

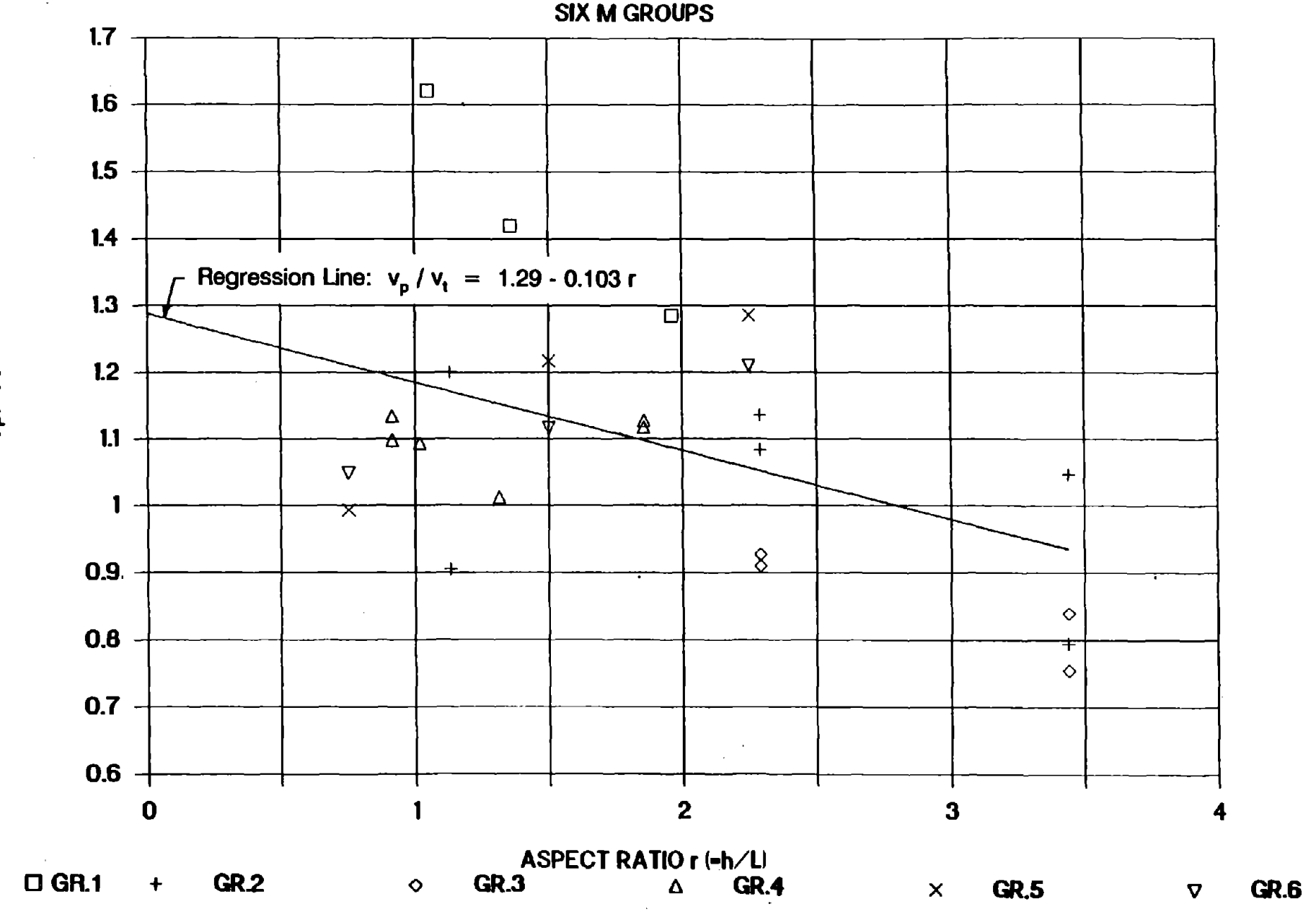

Figure 11. Effect of ph on strength

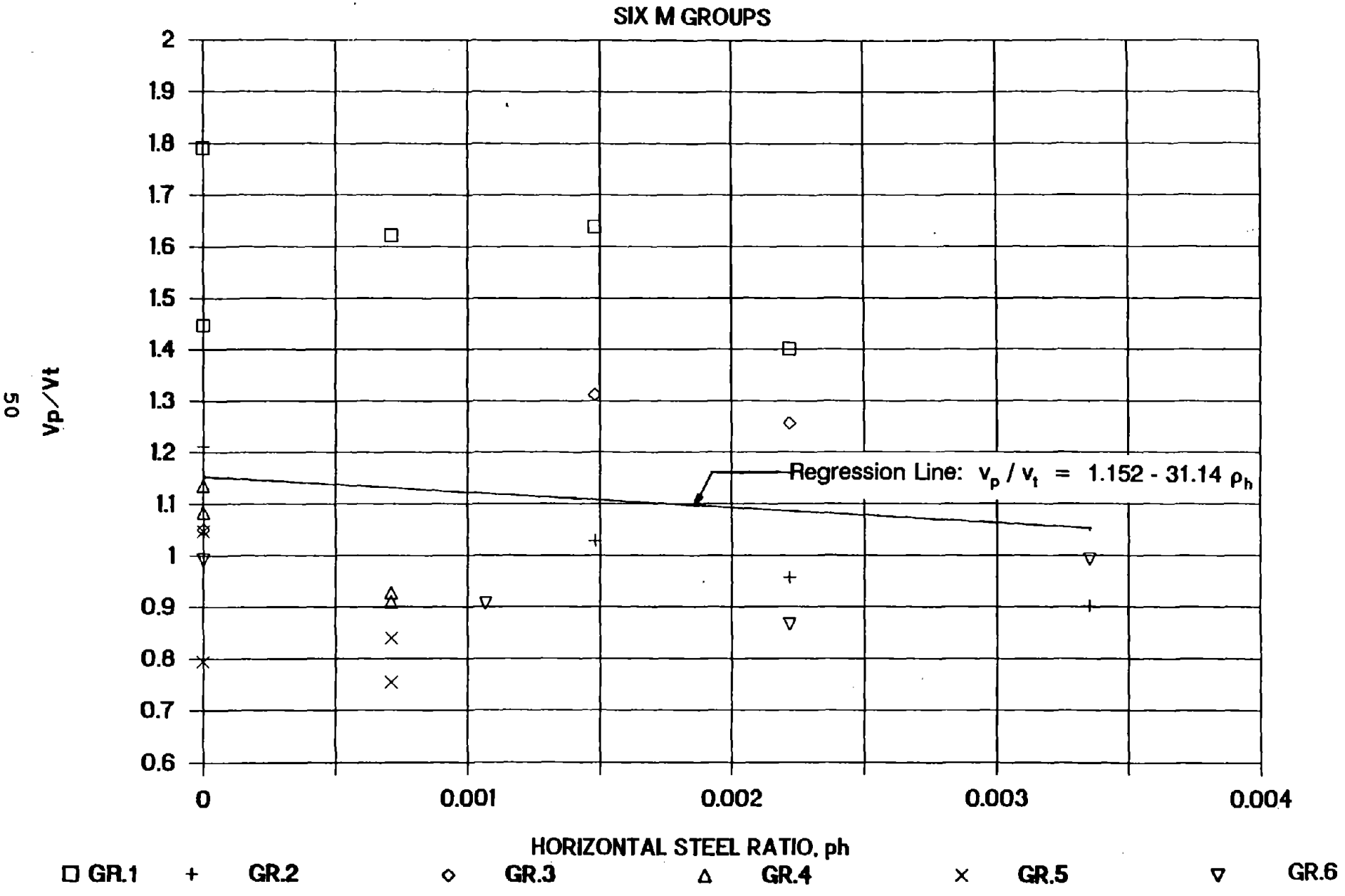

Figure 12. Effect of fm on strength

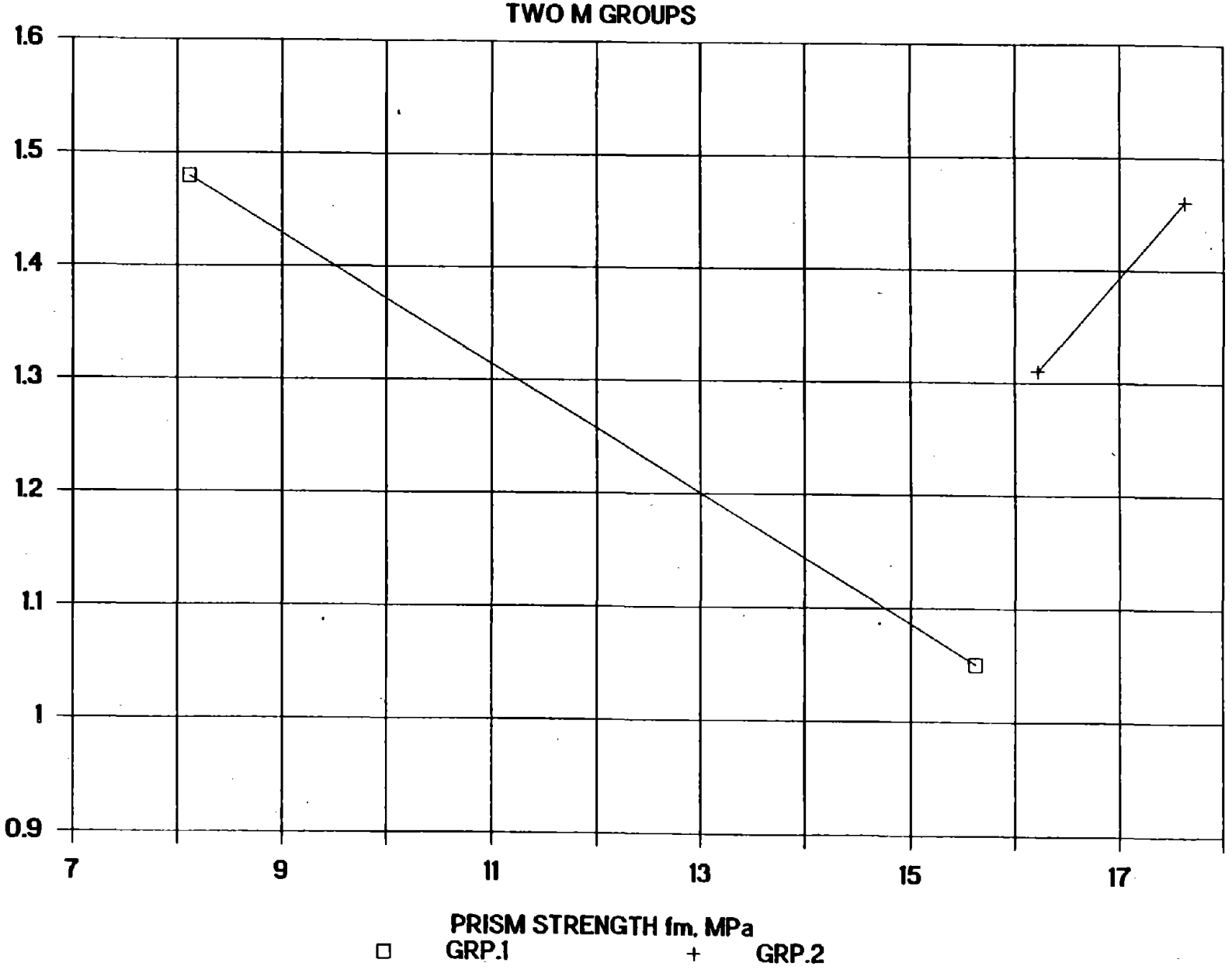

Figure 13. Strength Ratios, data set M

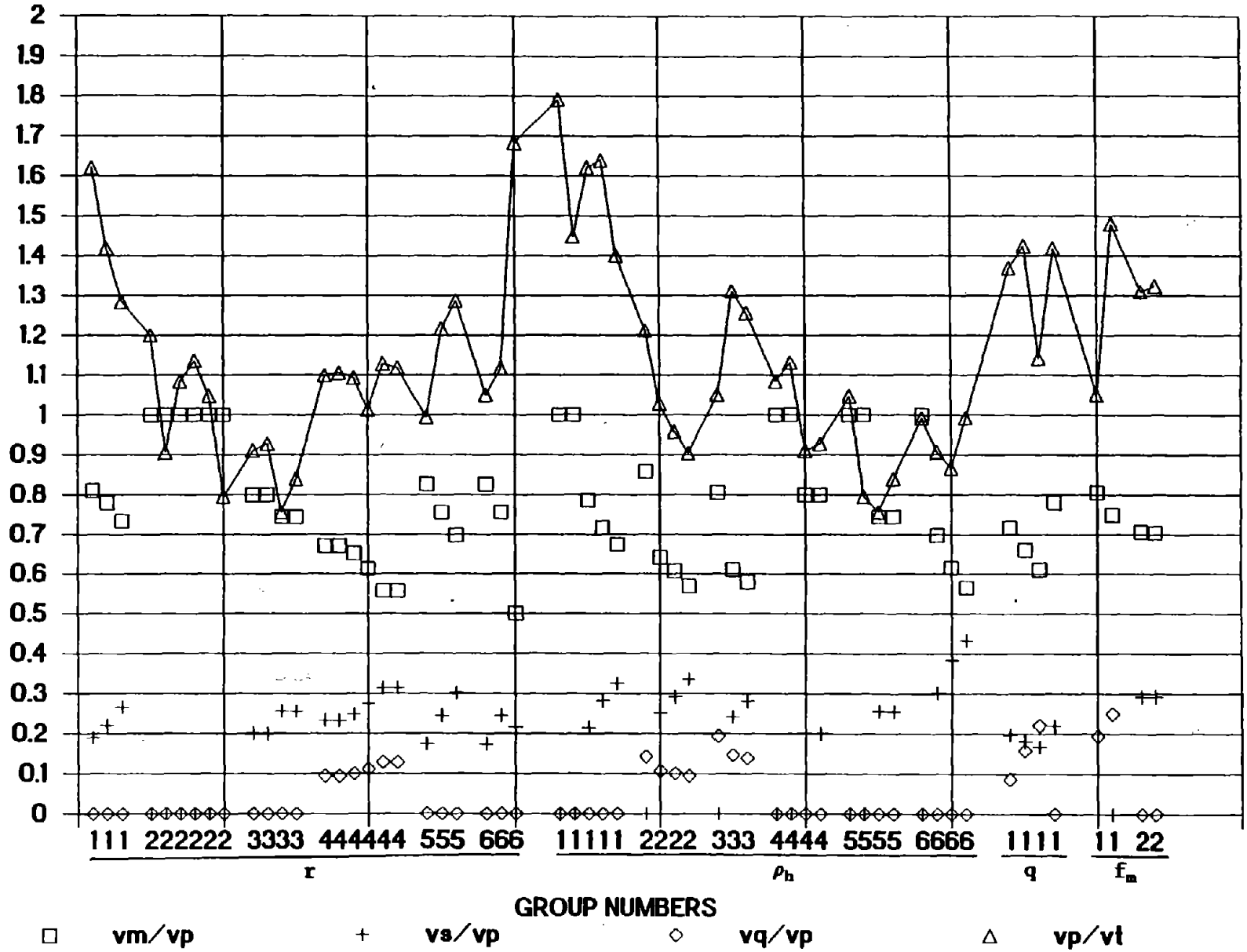

Figure 14. vp/vt ratio, Eq. (1)

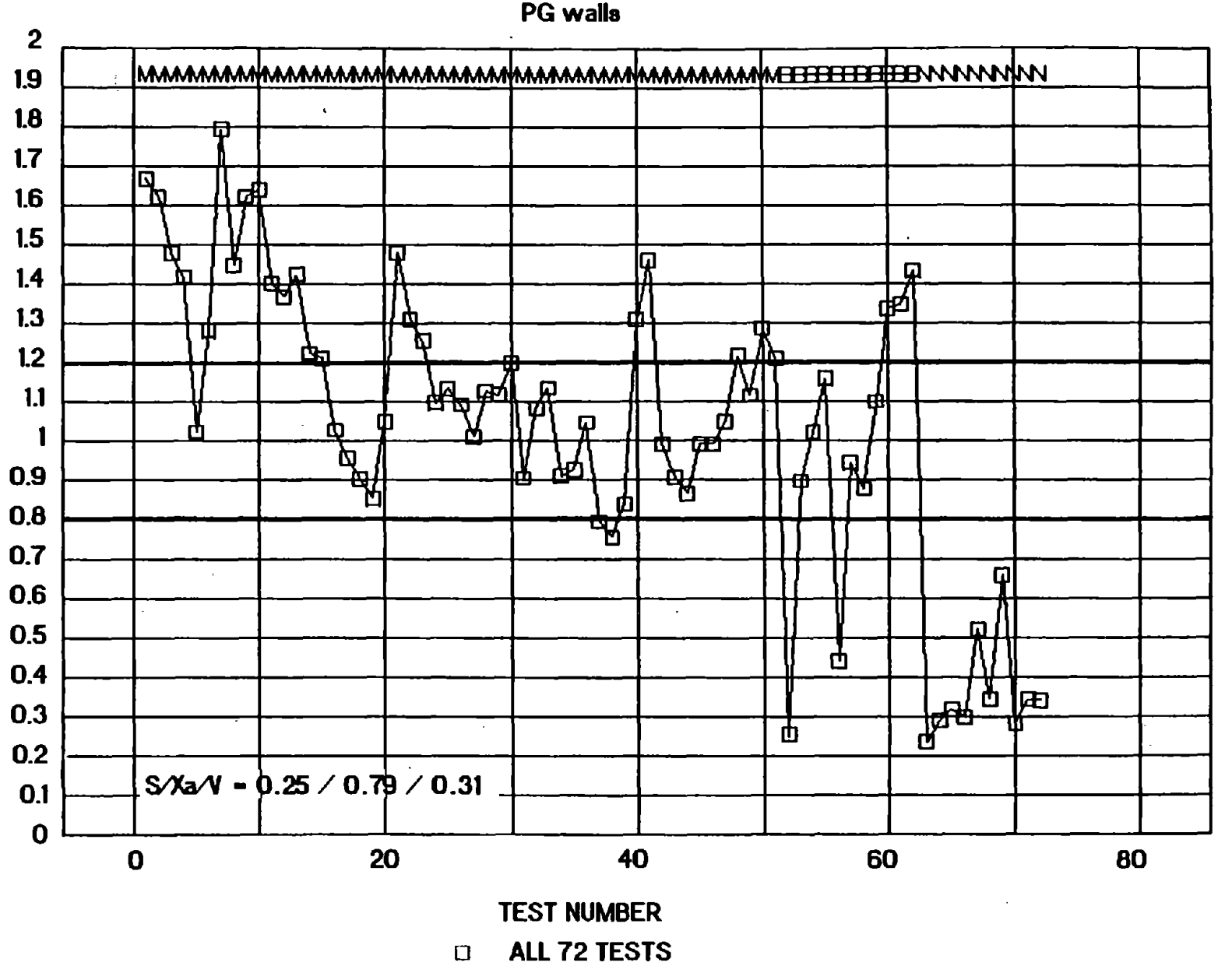

Figure 15. vp/vt ratio, Eq. (6)

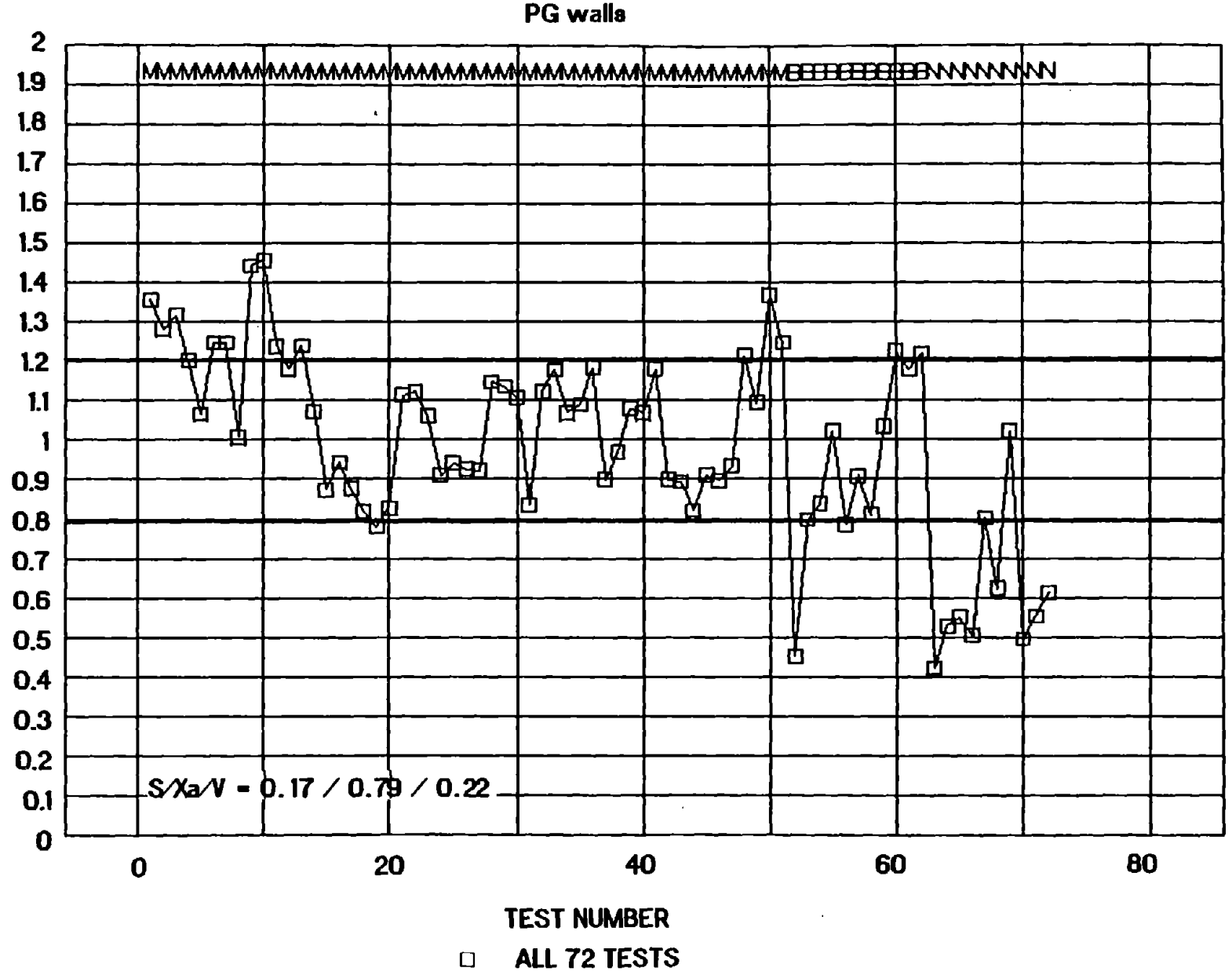

Figure 16. vp/vt ratio, Eq. (1)

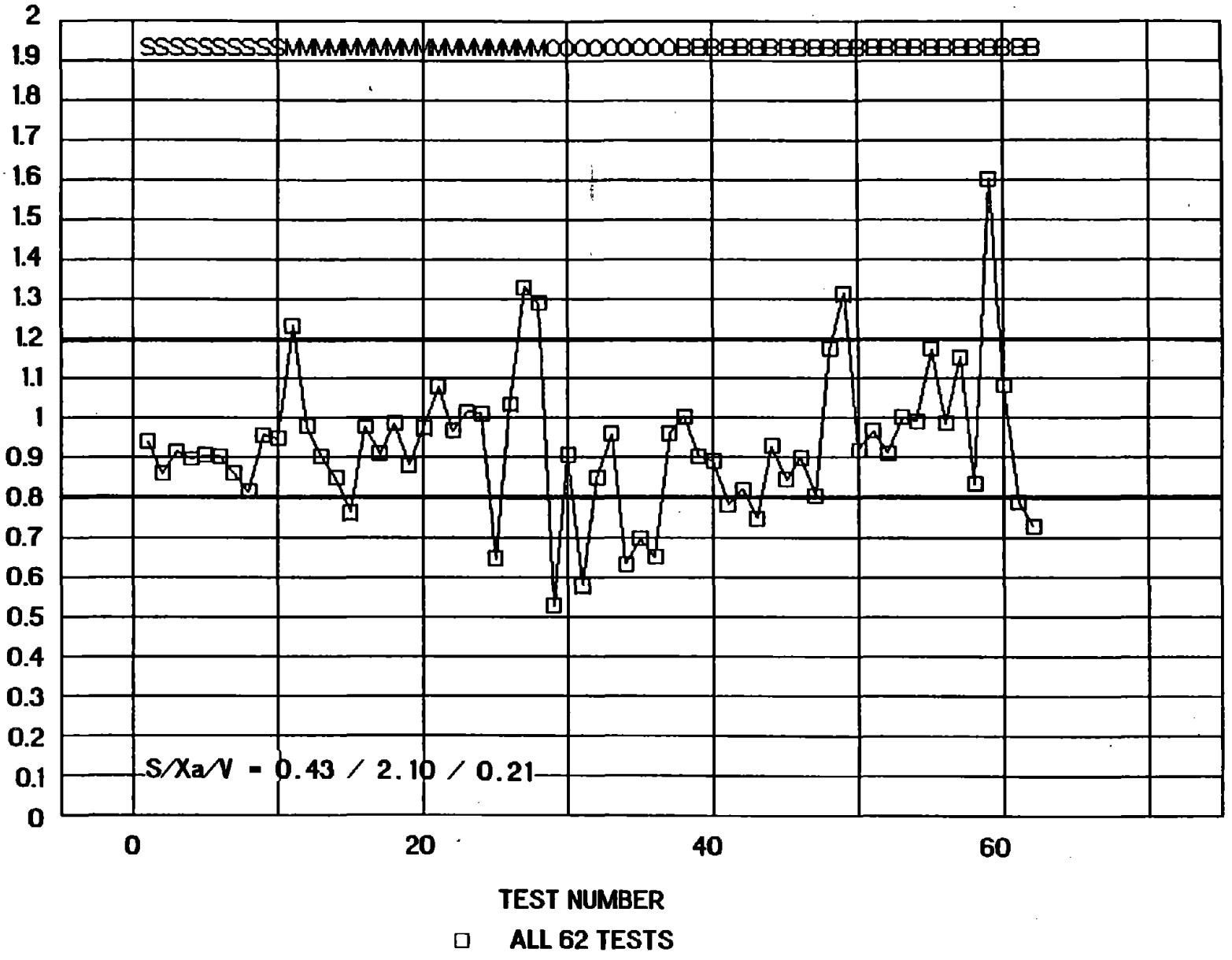

Figure 17. vp/vt ratio, Eq. (6)